Who Counts as Young? Matching Rules for Social Discounting[1]

I. Sebastian Buhai[2]

SOFI, Stockholm University

Instituto de Economia, UC Chile

NIPE, University of Minho

This version: June 2, 2026. Latest version.

Abstract

In heterogeneous OLG economies, age alone does not tell us who counts as young or old in a local welfare comparison. For such a comparison to have normative content, it must specify the represented margin, the private unit of account, the current information that identifies the relevant cell, and the common support over which claims are made. This paper provides that discipline. It separates raw resource weights from residual weights expressed in private value units, and shows that imposed local discount labels are valid precisely when they are induced by a potential on the graph. A calibrated audit of an OLG model then maps the frontier of certified claims, with support, units, wedges, and anchors determining which welfare signs are justified.

Keywords. Social discounting; intergenerational welfare; overlapping generations; heterogeneous agents; welfare weights; common support; current-cell matching; graph rationalizability

JEL Codes. D61, D63, D15, D52, E21, H43, C63

[1]I used Refine.ink, developed by Ben Golub and Yann Calvó López, to audit notational consistency and proof clarity. All remaining errors are my own. Replication files for the quantitative exercise are available in the project's GitHub repository at https://github.com/sbuhai/current-cell-matching-project.

[2]Email: sebastian.buhai@sofi.su.se. Website: sebastianbuhai.com

1 Introduction

Who is the young person in a local social discounting comparison? In a representative agent model, or in an overlapping generations (OLG) model in which age is the only state, the question hardly arises. In a heterogeneous life cycle economy it is central. Young agents differ in assets, earnings, constraints, health, continuation values, and private marginal values of current resources. Choosing one cell rather than another therefore changes the welfare object before any ethical view about age or time has been imposed.

Comparing by age alone has content only after that object is fixed. One may ask how the planner values an extra physical unit at two cells. One may instead express the unit in terms of private marginal value. Or one could ask, in physical resource units, whether age still carries social priority once the information that matters for the current margin, apart from age, and the private unit are held fixed. Table 1 below makes these distinctions explicit.

The diagnostic I propose here targets the last object. Fix a represented margin, such as saving over one period, and fix the private unit. Record the information, apart from age, that prices that margin, together with the private marginal value of current resources. Young and old cells are compared only where both are supported. When that information and that value coincide, any remaining difference in the planner's valuation is residual social priority measured in physical resources. Coarser comparisons can still answer other questions. They acquire the residual interpretation only under this current cell discipline.

Given these admissible comparisons, the formal restriction is a potential condition on a graph. Vertices are supported cells at the current date; edges are young to old comparisons that pass the bridge test. Edge labels combine the market compensation factor, the imposed social discount schedule, and KKT or bridge corrections. A local schedule is rationalizable by positive residual multipliers exactly when parallel witnesses agree and all cycle sums vanish. Residual levels are then identified up to one multiplicative constant in each connected component. The graph lemma itself is standard; the novelty herein lies in the economic construction that gives meaning to its vertices, labels, support, units, bridges, and anchors.

The bridge is explicit. The baseline is nonpaternalistic on the represented margin: conditional on the current marginal weights, the planner respects the individual's private ranking of the represented

future leg. KKT loadings enter as implementability wedges. If paternalism, survival, health, or other continuation concerns give that future leg additional ethical weight, the corresponding adjustment enters the bridge term. The theorem is conditional on the declared bridge, and the numerical audit reports a bounded frontier over such corrections.

My quantitative exercise uses this machinery as a certification audit in a calibrated heterogeneous agent OLG economy. The focal target compares ages 25 to 34 in the central row for current earnings with ages 45 to 54 on the same represented margin. The exercise reports a frontier rather than a point estimate, asking whether the sign attached to age survives comparisons within the same current cell. Intervals based on age alone include 0. Under the exhaustive tolerance graph, the interval is negative when the anchor is fixed. If anchors are allowed to vary freely across components, the supported normalized contrast in residual multipliers is not identified; on the largest common component, the local interval is positive. The fixed anchor result therefore reflects normalization across components and unequal exposure of the target cells, and it is fully consistent with the restriction that every admissible edge tilts toward younger agents.

The study's contribution is therefore not another age ranking for a heterogeneous model, but a discipline for interpreting age signs: when local discount labels can be represented by residual multipliers, when a sign is certified by supported model comparisons, and when it instead rests on support, units, wedges, or anchors.

The natural benchmark is Eden (2023), who derives an implication of social discounting across ages in the cross section. I keep the logic linking current allocations to continuation values, but add the step that heterogeneity makes unavoidable: the young and old cells to be compared must be specified, and that choice is part of the welfare object. The paper also relates to social discounting and OLG analyses including Caplin and Leahy (2004), Calvo and Obstfeld (1988), Farhi and Werning (2007), Feng and Ke (2018), Mertens and Rubinchik (2012), Howarth and Norgaard (1993), Schneider et al. (2012), Karp and Rezai (2014), and Millner and Heal (2023). Relative to this literature, the primitive issue is interpretability: age comparisons do not speak for themselves, and the question is when they can be read as comparisons of residual priority.

The same issue distinguishes the paper from welfare accounting in heterogeneous agent economies. Dávila and Schaab (2025), Barcons et al. (2026), and Baqaee et al. (2024) evaluate welfare once perturbations and money metrics have been chosen. Here, the comparison itself is disciplined first:

its support, unit, and residual priority interpretation are fixed before aggregation. The private unit is an interpersonal comparability convention in the sense of Harsanyi (1955). The support requirement parallels the common support discipline in matching and program evaluation (Heckman et al., 1997; Imbens and Wooldridge, 2009), with both support and units part of the estimand, not details of implementation. Generalized marginal welfare weights (Saez and Stantcheva, 2016; Sher, 2024) and marginal value of public funds valuation (Hendren and Sprung-Keyser, 2020) are complementary tools once that estimand has been defined.

The rest of the paper proceeds as follows. Section 2 gives the object taxonomy, example, and current-cell rule. Sections 3 and 4 define the environment, weights, private unit, and exact fibers. Sections 5 and 6 derive the pairwise decomposition and bridge. Section 7 gives supported graphs, rationalizability, approximate bands, and component anchors. Section 8 implements the quantitative certification audit. I collect aggregation details and proofs in the paper's appendix.

2 Object Taxonomy and Current-Cell Rule

The mechanism is clearest before the full environment is introduced. Eden's benchmark compares an old agent today with a young agent today, valuing the young agent at the date when she reaches the old agent's age. Heterogeneity makes that comparison incomplete unless four objects at the current date are fixed: the represented margin, the information other than age that prices that margin, the private unit, and the common support on which young and old cells can be paired.

2.1 What is being compared?

Table 1: Three local welfare objects

Welfare object	Compares	Exact current-cell matching?	Interpretation
Raw resource weight ω	Social value of one physical resource unit	No	A valid resource-weight comparison; mixes residual priority and private marginal value.
PVEU residual weight $\eta = \omega/\upsilon$	Social value of one private-value-equivalent unit	Requires a private-unit convention	Removes private marginal-value levels but remains indexed by the chosen private scale.
Residual priority in physical-resource units	Resource weights holding fixed χ and υ	Yes	Isolates residual social priority on the represented margin and common support.

Age-only matching is meaningful once the column of Table 1 is stated. Current-cell matching supplies the discipline needed for the residual-priority physical-resource object. Raw resource and PVEU comparisons retain their own economic content.

2.2 A numerical two-cell problem

At date t, let o be an old cell and let y_L, y_H be feasible same-age young cells. Suppose

$$(\omega_t, \upsilon_t, \eta_t)(o) = (6, 2, 3), \qquad (\omega_t, \upsilon_t, \eta_t)(y_L) = (8, 4, 2), \qquad (\omega_t, \upsilon_t, \eta_t)(y_H) = (4, 1, 4).$$

Raw-resource comparisons contradict: matching o with y_L favors the young ($8 > 6$), while matching o with y_H favors the old ($4 < 6$). In PVEU units, the residual weights are 2, 3, and 4; the comparison with y_L favors the old, while the comparison with y_H favors the young. The ordering changes because the private unit and the current cell have changed, before any ethical age judgment is imposed.

2.3 Current-cell matching

Fix a represented self-transfer margin M. Let $\chi_t^M(x)$ collect the non-age current information needed to determine the represented future leg, the market compensation factor, and the KKT loadings for that margin. The exact current-cell fiber is

$$\mathcal{F}_t^M(u, v) = \{x : \chi_t^M(x) = u,\ \upsilon_t(x) = v\}.$$

Two current cells can be compared as residual-priority physical-resource comparisons on margin M only when they lie in the same fiber. Exact fibers are the conceptual diagnostic benchmark. Finite-grid applications use tolerance bands in $|\Delta \log \upsilon|$, build intervals, and use K-nearest search as a computational device for finding candidates inside the tolerance set.

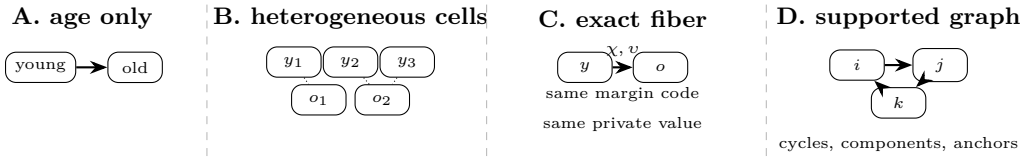

Figure 1: Current-cell matching replaces age-only labels with economically verified vertices, support, edge labels, cycles, and component anchors.

2.4 A first concrete map: one-step saving

The leading example is a finite-life one-asset household with state $x = (a, b, \varepsilon_k)$. For the represented one-step risk-free saving margin,

$$u'(c_a(b, \varepsilon_k)) = \beta p_a (1 + r) \sum_{k'} P_{kk'} u'(c_{a+1}(b'_a(b, \varepsilon_k), \varepsilon_{k'})) + \mu_a(b, \varepsilon_k), \tag{1}$$

where p_a is survival, P is the earnings transition matrix, and $\mu_a \geq 0$ is the borrowing multiplier. The private envelope is

$$\upsilon_a(b, \varepsilon_k) = u'(c_a(b, \varepsilon_k)). \tag{2}$$

Provided the private envelope is one-to-one in the scalar resource state within a transition-row class, equality of υ_a identifies that resource state. The transition row then fixes the continuation composition apart from age. For this one-step saving margin, the verified current code is therefore

the transition-row type.

Table 2: Margin-sufficiency certificate for current maps

Margin	Represented leg	Market object	Current loading	Required non-age code χ^M
Risk-free saving	next-period survival-contingent asset payoff	$1+r$	borrowing/Euler wedge	transition-row type
Risky asset	state-contingent payoff vector	asset price/state-price vector	portfolio constraints	payoff regime and transition row
Labor-tax margin	current labor/resource perturbation	after-tax wage	labor wedge	productivity, earnings, and tax regime
Liquid/illiquid saving	liquid and illiquid portfolio leg	asset prices and adjustment cost	portfolio/adjustment constraints	illiquid state, adjustment regime, and transition row

The notation below has the following identification content. The represented margin M and private unit υ_t are maintained. The current map χ_t^M is verified from the represented margin. The market factor $\mathcal{Q}$ and KKT wedge Λ are computed from that margin; the imposed schedule $\bar{\mathcal{D}}^S$ is tested. Components are computed from graph support, residual multipliers η_t are recovered as graph potentials within components, and cross-component anchors are maintained when target mass lies in disconnected components.

2.5 Relation to adjacent welfare frameworks

The relation to heterogeneous-agent welfare accounting is one of inputs rather than substitutes. Dávila and Schaab (2025), Barcons et al. (2026), and Baqaee et al. (2024) evaluate welfare for specified perturbations, weights, and numeraires. I examine the comparison that supplies such inputs: which cells, margin, unit, bridge, and support make an age sign interpretable as residual social priority. Once these objects fixed, resulting multipliers can enter standard accounting exercises; w/out them, an age sign may reflect states, units, wedges, or anchors rather than priority by age.

3 Environment

This section fixes the demographic environment, admissible perturbations, and attainable self-transfer correspondence used in the bridge.

3.1 Demographic structure and uncertainty

Time is discrete, $t \in \mathbb{Z}_+$. The benchmark aggregate path is deterministic; uncertainty indexes idiosyncratic histories. Each period a cohort is born. Ages are $a \in \mathcal{A} = \{0, 1, \ldots, A\}$. An individual's state is $z \in \mathcal{Z}$, a Borel subset of Euclidean space; it may include assets, productivity, health, promised utility, or any state needed for private choices and social comparisons. A cell is $x = (a, z) \in \mathcal{X} := \mathcal{A} \times \mathcal{Z}$.

At date t, the living cross section is the probability measure μ_t on $\mathcal{X}$. The benchmark path is $\{\mu_t, c_t, p_t\}_{t\geq 0}$, where $c_t(x)$ is the private allocation and p_t collects prices, taxes, transfers, and aggregate objects.

3.2 Private behavior, continuation support, and attainable self-transfers

Individuals optimize given benchmark prices, policies, and constraints. For $s \geq t$ and current living cell x, let $\Gamma_{t,s}(x) \subseteq \mathcal{X}$ be the support of the date-s living-cell law conditional on survival to s when survival has positive probability, and set it to $\emptyset$ otherwise; represented future legs carry survival probabilities.

For $y \in \Gamma_{t,s}(x)$, an attainable set

$$\mathcal{T}_{t,s}(x, y) \subseteq \mathbb{R}^2_+$$

contains pairs (δ_t, δ_s) such that surrendering δ_t date-t units at x can finance δ_s units at date s in cell y through benchmark opportunities along the same individual history. On bridge-verified tuples the normalized exchange frontier $\sup\{\delta_s/\delta_t : (\delta_t, \delta_s) \in \mathcal{T}_{t,s}(x, y),\ \delta_t > 0\}$ is finite and positive and the attainable graph is measurable; otherwise the tuple is unsupported.

Assumption 3.1 (Admissible benchmark path)**.** The benchmark path is feasible, measurable, and implementable. Conditional on age, z is sufficient for the local continuation problem; $\Gamma_{t,s}$ is measurable for every $s \geq t$; and the benchmark allocation solves the individual's problem given prices and constraints.

3.3 Local perturbations

A benchmark perturbation path is a feasible family of resource top-up schedules $m^\tau_t : \mathcal{X} \to \mathbb{R}$ around the benchmark, with fixed prices, policies, survival laws, transition laws, and μ_t unless an extension

declares a general-equilibrium object. Its first-order signed resource shift is $\Delta = \{\Delta_t\}_{t\geq 0}$.

Definition 3.2 (Admissible perturbation)**.** A signed finite-horizon perturbation Δ is *admissible* if:

(i) Δ_t is absolutely continuous with respect to μ_t, with density $h_t \in L^\infty(\mu_t)$ for every t;

(ii) Δ is the two-sided first-order resource shift generated by a feasible benchmark perturbation path; and

(iii) the relevant social and private Gâteaux derivatives along Δ exist.

Assumption 3.3 (Localized cell evaluation)**.** On finite grids, displayed cell shifts are cell-level resource-rate shifts, the density values $h_t(x)$ in $\Delta_t(\mathrm{d}x) = h_t(x)\mu_t(\mathrm{d}x)$, and not changes in population mass or unnormalized aggregate cell resources. On continuous supports, fix the Euclidean diferentiation basis on the Borel state coordinates, or any stated standard differentiation basis. A displayed shift at a cell is the limit, when it exists, of admissible perturbations with uniformly bounded densities, supported on neighborhoods that shrink to the cell under the chosen differentiation basis, after normalization by the μ_t-measure of the neighborhood. It is a derivative per unit of local mass, not a shift of the neighborhood as a whole. Identities involving $(\omega_t, \upsilon_t, \eta_t)$ are asserted after fixing versions of these objects on sets of full measure; absent such versions, they are understood as identities in the relevant conditional essential range.

3.4 Valuation systems

Social valuation is the directional derivative of the planner's objective. Private valuation is summarized by the private envelope derivative $\upsilon_t(x)$ and, for attainable self-connected perturbations, by market compensation factors or supporting state-price factors. Once a common private unit is fixed, the residual object is $\eta_t(x) = \omega_t(x)/\upsilon_t(x)$; the current comparison map decides which residual ratios are exact-fiber comparisons.

4 Weights, Units, and Current-Cell Fibers

This section defines raw physical-resource weights, private-value-equivalent weights, and exact-fiber residual comparisons. Exact fibers add equality of the margin-sufficient current code and private envelope, so physical-resource comparisons isolate residual social priority.

4.1 Local derivatives

Assumption 4.1 (Local differentiability and positivity)**.** For every admissible perturbation Δ, write $\Delta_t(\mathrm{d}x) = h_t(x)\mu_t(\mathrm{d}x)$. The social objective admits the Gâteaux derivative

$$D\mathcal{W}[\Delta] = \sum_{t\geq 0} \int_{\mathcal{X}} \omega_t(x) h_t(x) \mu_t(\mathrm{d}x)$$

for some measurable $\omega_t : \mathcal{X} \to (0, \infty)$, defined μ_t almost everywhere, with finite displayed integrals on the admissible bounded-density domain. The tangent space is dated-separating: if $\sum_t \int f_t h_t \, \mathrm{d}\mu_t = 0$ for every admissible finite-horizon perturbation, then $f_t = 0$ μ_t almost everywhere on each active date. For each active t and μ_t almost everywhere x, a private continuation value $V_t(x; m)$ is differentiable at current-resource top-up $m = 0$, with

$$\upsilon_t(x) := \left.\frac{\partial V_t(x; m)}{\partial m}\right|_{m=0} \in (0, \infty).$$

Definition 4.2 (Social marginal welfare weight)**.** The *social marginal welfare weight* is any measurable representer $\omega_t(x)$ satisfying, for every admissible Δ,

$$D\mathcal{W}[\Delta] = \sum_{t\geq 0} \int_{\mathcal{X}} \omega_t(x) h_t(x) \mu_t(\mathrm{d}x). \tag{3}$$

It is unique up to μ_t-null sets by dated separation.

Definition 4.3 (Normalized residual multiplier)**.** Under Assumptions 3.1 and 4.1, define

$$\eta_t(x) := \frac{\omega_t(x)}{\upsilon_t(x)}. \tag{4}$$

Lemma 4.4 (Factorization and scale properties)**.** *On* $\{\upsilon_t > 0\}$*,*

$$\omega_t(x) = \eta_t(x)\upsilon_t(x). \tag{5}$$

If the private utility index is transformed everywhere by $u \mapsto \alpha u + \beta$*,* $\alpha > 0$*, while the planner's cardinal representation over physical allocations is fixed, then* υ_t *scales by* α*,* ω_t *is unchanged, and* η_t *scales by* α^{-1}*. Cross-cell ratios of* η *are invariant to common positive affine rescaling.*

Proof. The identity is the definition of η_t. A common rescaling multiplies every private envelope derivative by the same α and leaves the social derivative with respect to physical resources unchanged, so residual ratios are unchanged. □

4.2 The maintained private unit

Assumption 4.5 (Common cardinal private scale)**.** Cross-cell comparisons of $\upsilon_t(x)$ use a maintained common cardinal indexing of the relevant private continuation problem. Common positive affine transformations are innocuous; cell-specific slope changes are not.

I maintain the private unit as an interpersonal-comparability convention in the sense of Harsanyi (1955). Every graph and numerical conclusion is indexed by (M, χ, υ): represented margin, margin-sufficient current map, private unit. Common affine rescaling leaves ratios of η unchanged. Cell-specific slopes change exact support because $\upsilon_i = \upsilon_j$ becomes $a_i\upsilon_i = a_j\upsilon_j$. An alternative admissible unit system requires rebuilding exact fibers, edges, components, support shares, edge labels, and anchors. The unit path in the quantitative audit reports this change in the identified object.

The maintained unit is current goods: $\omega_t(x)$ prices physical top-ups in the planner's feasibility constraint. Taxes, transfers, and compensations use goods or dollars, not cell-specific private-value indices. A common private scale is therefore a Harsanyi convention over the same physical perturbation; a cell-specific rescaling changes the perturbation metric and exact-fiber relation, so it is a different object, not a harmless numeraire change.

4.3 Private value equivalent units

Definition 4.6 (Private value equivalent unit)**.** When $0 < \upsilon_t(x) < \infty$, one *private-value-equivalent unit*, or PVEU, at (t, x) is the local resource shift of size $1/\upsilon_t(x)$.

A PVEU raises private continuation value by one marginal unit. An admissible Δ is PVEU-integrable when $\sum_t \int \upsilon_t \, \mathrm{d}|\Delta_t| < \infty$ over active dates.

Proposition 4.7 (PVEU representation)**.** *For any* PVEU*-integrable admissible* Δ*, define*

$$\Delta_t^{\mathrm{PVEU}}(\mathrm{d}x) := \upsilon_t(x)\Delta_t(\mathrm{d}x).$$

Then

$$DW[\Delta] = \sum_{t\geq 0} \int_{\mathcal{X}} \omega_t(x)\Delta_t(\mathrm{d}x) = \sum_{t\geq 0} \int_{\mathcal{X}} \eta_t(x)\Delta_t^{\mathrm{PVEU}}(\mathrm{d}x). \tag{6}$$

Thus $\eta_t(x)$ is the social value of one PVEU *delivered to cell x on this integrable local domain.*

Proof. Substitute $\omega_t = \eta_t \upsilon_t$ into Equation (3) and use the definition of Δ_t^{PVEU}. □

For cells with positive private marginal values,

$$\frac{\omega_t(x)}{\omega_t(x')} = \frac{\upsilon_t(x)}{\upsilon_t(x')}\frac{\eta_t(x)}{\eta_t(x')}.$$

PVEU weights allow unequal private marginal values; exact fibers diagnose residual priority in physical-resource units.

4.4 Comparison maps and fibers

For margin M, let $Z_t^M(x)$ collect the non-age current primitives identifying the continuation leg, gross market compensation, and loading constraints. Deterministic age schedules remain part of the age comparison.

Definition 4.8 (Margin sufficient comparison map)**.** Fix a represented local margin class M at date t. A measurable map $\chi_t : \mathcal{X} \to \mathcal{U}$ is *margin-sufficient* for M if it uses a common non-age coding across age slices and, whenever $x = (a, z)$ and $x' = (a', z')$ satisfy $\chi_t(x) = \chi_t(x')$ and $\upsilon_t(x) = \upsilon_t(x')$ in a represented tuple, the tuple's age alignment identifies the non-age objects determining: (i) admissibility and valuation of the represented future leg; (ii) $\mathcal{Q}$; and (iii) the current loadings entering Λ. A verification certificate lists the primitive leg, price, and loadings; any coarsening requires a new sufficiency check.

The verification certificate is primitive: list the represented leg, price object, and loadings, then keep the non-age coordinates needed to identify them once age alignment and υ_t are fixed. The compact certificate in Table 2 gives the benchmark saving, risky-asset, labor-tax, and liquid/illiquid cases. Coarsening the map demands a new sufficiency check.

Proposition 4.9 (Verified margin sufficiency discipline)**.** *Fix M and suppose a minimal verified margin-sufficient map χ_t^M has been constructed on the maintained support, where minimality is*

ordered by partition refinement of the admissible current-pair relation.

(i) Exact fiber matching on (χ_t^M, υ_t) holds fixed all non-age current state objects needed to interpret M; age-dependent deterministic schedules may vary.

(ii) A coarsening $\widetilde{\chi}_t$ that merges same-age cells with equal υ_t but different verified codes requires a new sufficiency check.

(iii) Any refinement $\bar{\chi}_t = (\chi_t^M, W_t)$ remains margin-sufficient and weakly shrinks admissible matches.

Definition 4.10 (Comparison fiber)**.** For a verified margin-sufficient map χ_t, date t, attribute $u \in \mathcal{U}$, and private envelope scale $v > 0$, the *comparison fiber* is

$$\mathcal{F}_t(u, v) := \{x \in \mathcal{X} : \chi_t(x) = u \text{ and } \upsilon_t(x) = v\}. \tag{7}$$

Cells in a verified fiber have the same represented current code and private marginal value. Physical resource transfers within such a fiber therefore compare η ratios as residual-priority comparisons; a coarsening has that interpretation only after its own sufficiency check.

Proposition 4.11 (Unit dependence requires graph rebuild)**.** *Under Assumptions 3.1, 4.1 and 4.5, common positive affine rescaling leaves every ratio of normalized residual multipliers unchanged. A cell-specific admissible rescaling can change υ_t, exact fibers, supported matches, edge labels, connected components, component anchors, and target intervals. Alternative private-unit conventions therefore requires recomputing the comparison graph.*

Proof. Common rescaling multiplies all private envelopes by the same constant and cancels from residual ratios. Cell-specific rescaling changes equality relations in Equation (7) and hence every object built from supported fibers. □

Lemma 4.12 (Exact fibers isolate residual priority)**.** *Fix M and a verified map χ_t^M. Among coordinate rules using (χ_t^M, υ_t), exact fibers are the minimal diagnostic rule, ordered by partition refinement, that preserves equality of raw-resource and residual-priority comparisons, is invariant to common private-scale rescaling, and deletes only the comparisons needed to enforce the private unit and verified current code.*

Proof. If a rule admits a pair with unequal v_t, then the raw ratio differs from the residual ratio by $v_t(x)/v_t(x')$, violating residual isolation. If it merges distinct verified codes, it abandons the verified margin sufficiency of M. The exact fiber imposes precisely these two equalities and is unchanged by common rescaling. □

Remark 4.13 (Weaker comparability). If the analyst has only partial cardinal comparability, the exact-fiber graph is indexed by that weaker unit system. All graph and interval statements remain conditional on the chosen unit.

Lemma 4.14 (Nonvacuity under a monotone matching state)**.** *Suppose that for two ages and a common verified code u, the scalar resource state $b \mapsto v_t(a, b, u)$ is continuous and strictly monotone on support intervals whose images overlap. Then every v in the overlap defines a nonempty cross-age exact fiber.*

4.5 Local scope and conditional residual age neutrality

Definition 4.15 (Conditional residual age neutrality relative to a comparison system)**.** Given a comparison system (M, χ, v), the social criterion is *conditionally residual-age neutral* on a set of exact comparison tuples if

$$\eta_t(x_t^{\mathrm{o}}) = \eta_t(x_t^{\mathrm{y}})$$

for each tuple in the set. The neutrality statement is local to the represented margin, verified current map, private unit, and support.

Remark 4.16 (Theorem, bound, and point-summary layers). Exact fiber tuples are theorem objects; ε-matched tuples add mismatch bounds; coarsened maps add contamination radius κ; finite-grid recursions choose point summaries inside these bounds. The numerical section reports intervals before point summaries.

5 Pairwise Decomposition under Current-Cell Matching

This section states the pairwise algebra. Exact fibers isolate the residual multiplier comparison. Coarser rules mix residual priority with current private scale, and approximate matching records

the resulting error. Longer horizons are first handled along a fixed chain; path independence across chains appears in Section 7.

5.1 Comparison tuples

Fix date t. Let x_t^{o} and x_t^{y} be current cells in the same comparison fiber, with $a^{\mathrm{o}} > a^{\mathrm{y}}$, and put $s = t + a^{\mathrm{o}} - a^{\mathrm{y}}$. If $x_s^{\mathrm{o}} \in \Gamma_{t,s}(x_t^{\mathrm{y}})$ has age a^{o}, the following object is admissible.

Definition 5.1 (Comparison tuple)**.** A *comparison tuple* is

$$\pi = (t, x_t^{\mathrm{o}}, x_t^{\mathrm{y}}, x_s^{\mathrm{o}})$$

such that (i) x_t^{o} and x_t^{y} lie at date t and in the same comparison fiber; (ii) $a(x_t^{\mathrm{o}}) > a(x_t^{\mathrm{y}})$; and (iii) $x_s^{\mathrm{o}} \in \Gamma_{t,s}(x_t^{\mathrm{y}})$ with $a(x_s^{\mathrm{o}}) = a(x_t^{\mathrm{o}})$.

Definition 5.2 (Ordered and baseline bridge-verified tuples)**.** An *ordered tuple* is a quadruple $(t, x_t^{\mathrm{o}}, x_t^{\mathrm{y}}, x_s^{\mathrm{o}})$ satisfying the same age ordering, alignment, and continuation condition, without imposing exact fiber equality. It is *admissible approximate* when the maintained current codes agree and the stated private-envelope mismatch bound holds. It is *baseline bridge-verified* when the represented family, supporting-price/KKT representation, and nonpaternalistic domain assumptions apply. Note that a nonbaseline bridge-verified tuple additionally carries the declared positive correction $\mathfrak{B}(\pi)$ introduced in Subsection 6.2.

Remark 5.3 (Portfolio-valued future legs). The displayed tuple uses a singleton continuation cell. For a finite-support represented leg $L_s^{\pi} = \sum_j \ell_j \delta_{x_{sj}}$, with survival and transition probabilities absorbed in ℓ_j, write

$$\mathcal{V}_s^{\omega}(\pi) := \sum_j \ell_j \omega_s(x_{sj}),$$

and set $\mathcal{V}_s^{\omega}(\pi) = \omega_s(x_s^{\mathrm{o}})$ in the singleton case. The corresponding $\mathcal{Q}(\pi)$ is the gross market compensation factor for that represented portfolio leg; the one-step risk-free margin uses this version.

Definition 5.4 (Gross social discount ratio)**.** For $\pi = (t, x_t^{\mathrm{o}}, x_t^{\mathrm{y}}, x_s^{\mathrm{o}})$, or its portfolio-leg version, define

$$\mathcal{D}^S(\pi) := \frac{\omega_t(x_t^{\mathrm{o}})}{\mathcal{V}_s^{\omega}(\pi)}. \tag{8}$$

It is the marginal number of represented future old-age leg units socially equivalent to one current old-age resource unit.

Timing and units. $\mathcal{D}^S(\pi)$ is a gross social discount ratio for the represented future leg; if $\mathcal{D}^S = 1+\rho^S$, then ρ^S is the corresponding net rate. $\mathcal{Q}(\pi)$ is the gross market compensation factor for the same represented leg, and $\Lambda(\pi)$ corrects for KKT implementability. A comparison is meaningfull only when the social ratio and market ratio price the same represented leg in the same private unit.

5.2 Exact fiber decomposition

Proposition 5.5 (Exact-fiber pairwise decomposition)**.** *For any comparison tuple π, define*

$$\mathcal{M}(\pi) := \frac{\eta_t(x_t^{\mathrm{o}})}{\eta_t(x_t^{\mathrm{y}})} \tag{9}$$

and

$$\mathcal{R}^S(\pi) := \frac{\omega_t(x_t^{\mathrm{y}})}{\mathcal{V}_s^{\omega}(\pi)}. \tag{10}$$

Then

$$\mathcal{D}^S(\pi) = \mathcal{M}(\pi)\mathcal{R}^S(\pi). \tag{11}$$

Proof. Using $\omega_t = \eta_t \upsilon_t$,

$$\mathcal{D}^S(\pi) = \frac{\eta_t(x_t^{\mathrm{o}})}{\eta_t(x_t^{\mathrm{y}})} \frac{\upsilon_t(x_t^{\mathrm{o}})}{\upsilon_t(x_t^{\mathrm{y}})} \frac{\omega_t(x_t^{\mathrm{y}})}{\mathcal{V}_s^{\omega}(\pi)}.$$

The middle ratio is one on an exact fiber. □

Exact fiber matching turns the current term into a ratio of residual multipliers. The remaining term is the within-person intertemporal comparison along the younger individual's continuation.

5.3 Coarser and approximate current matching

A coarser rule may hold fixed only the state attribute and allow different υ_t values. The identity is exact; an error bound arises when private-scale mismatch is controlled.

Proposition 5.6 (Current scale contamination under coarser matching)**.** *Fix an ordered tuple $\bar{\pi} = (t, x_t^{\mathrm{o}}, x_t^{\mathrm{y}}, x_s^{\mathrm{o}})$ with $a(x_t^{\mathrm{o}}) > a(x_t^{\mathrm{y}})$, $s = t + a(x_t^{\mathrm{o}}) - a(x_t^{\mathrm{y}})$, $x_s^{\mathrm{o}} \in \Gamma_{t,s}(x_t^{\mathrm{y}})$, and $\chi_t(x_t^{\mathrm{o}}) = \chi_t(x_t^{\mathrm{y}})$,*

without imposing equality of υ_t. Then

$$\mathcal{D}^S(\bar{\pi}) = \frac{\eta_t(x_t^{\mathrm{o}})}{\eta_t(x_t^{\mathrm{y}})} \frac{\upsilon_t(x_t^{\mathrm{o}})}{\upsilon_t(x_t^{\mathrm{y}})} \mathcal{R}^S(\bar{\pi}), \tag{12}$$

or equivalently

$$\log \frac{\eta_t(x_t^{\mathrm{y}})}{\eta_t(x_t^{\mathrm{o}})} = \log \mathcal{R}^S(\bar{\pi}) - \log \mathcal{D}^S(\bar{\pi}) + \log \frac{\upsilon_t(x_t^{\mathrm{o}})}{\upsilon_t(x_t^{\mathrm{y}})}. \tag{13}$$

Corollary 5.7 (Approximate matching bound)**.** *Under Proposition 5.6, if*

$$|\log \upsilon_t(x_t^{\mathrm{o}}) - \log \upsilon_t(x_t^{\mathrm{y}})| \leq \varepsilon,$$

then

$$\left| \log \frac{\eta_t(x_t^{\mathrm{y}})}{\eta_t(x_t^{\mathrm{o}})} - \left(\log \mathcal{R}^S(\bar{\pi}) - \log \mathcal{D}^S(\bar{\pi}) \right) \right| \leq \varepsilon. \tag{14}$$

Equivalently,

$$\log \frac{\eta_t(x_t^{\mathrm{y}})}{\eta_t(x_t^{\mathrm{o}})} \geq \log \mathcal{R}^S(\bar{\pi}) - \log \mathcal{D}^S(\bar{\pi}) - \varepsilon, \tag{15}$$

$$\log \frac{\eta_t(x_t^{\mathrm{y}})}{\eta_t(x_t^{\mathrm{o}})} \leq \log \mathcal{R}^S(\bar{\pi}) - \log \mathcal{D}^S(\bar{\pi}) + \varepsilon. \tag{16}$$

When $\varepsilon = 0$, the exact fiber identity obtains.

Proposition 5.8 (Ordering ambiguity under coarse matching)**.** *For any $\gamma > 0$ and $\delta > \gamma$, there is an admissible local environment and a coarse current tuple $\bar{\pi}$ with common comparison attribute such that*

$$\log \mathcal{R}^S(\bar{\pi}) - \log \mathcal{D}^S(\bar{\pi}) = \gamma, \qquad \log \frac{\upsilon_t(x_t^{\mathrm{o}})}{\upsilon_t(x_t^{\mathrm{y}})} = -\delta,$$

and therefore

$$\log \frac{\eta_t(x_t^{\mathrm{y}})}{\eta_t(x_t^{\mathrm{o}})} = \gamma - \delta < 0. \tag{17}$$

Any exact fiber tuple with the same $\mathcal{R}^S$ and $\mathcal{D}^S$ satisfies $\log(\eta_t(x_t^{\mathrm{y}})/\eta_t(x_t^{\mathrm{o}})) = \gamma > 0$. Coarse matching can overturn the inferred age tilt.

5.4 Multiplication along a fixed exact fiber chain

For a chain of exact fiber comparison tuples $\{\pi_\ell\}_{\ell=0}^{n-1}$, define

$$\mathcal{D}^S(\pi_{0:n-1}) := \prod_{\ell=0}^{n-1} \mathcal{D}^S(\pi_\ell).$$

Corollary 5.9 (Blockwise multiplication on a fixed chain)**.** *For any exact fiber comparison tuples $\{\pi_\ell\}_{\ell=0}^{n-1}$, singleton or finite-portfolio future legs,*

$$\mathcal{D}^S(\pi_{0:n-1}) = \prod_{\ell=0}^{n-1} \mathcal{M}(\pi_\ell)\mathcal{R}^S(\pi_\ell). \tag{18}$$

If every future leg is a singleton and, for each $\ell < n-1$, the dated future older cell in block ℓ is the dated current older cell in block $\ell+1$, then with $(t_n, x^{\mathrm{o}}_{t_n,n}) = (s_{n-1}, x^{\mathrm{o}}_{s_{n-1},n-1})$,

$$\mathcal{D}^S(\pi_{0:n-1}) = \frac{\omega_{t_0}(x^{\mathrm{o}}_{t_0,0})}{\omega_{t_n}(x^{\mathrm{o}}_{t_n,n})} = \prod_{\ell=0}^{n-1} \mathcal{M}(\pi_\ell)\mathcal{R}^S(\pi_\ell). \tag{19}$$

Portfolio-valued legs retain the product form; linkwise bounds multiply and log errors add.

Remark 5.10 (Scope of the fixed-chain identity). Corollary 5.9 is a fixed-chain product identity. Proposition 7.6 concerns the stronger residual graph potential for $\log \eta$; finite-grid recursions are graph-specific once exact equality in υ_t is replaced by approximate matching.

Remark 5.11 (Relation to Eden's age-based benchmark). Suppressing υ_t from the current rule leaves the coarser same-χ_t rule. Pure age matching arises when the margin code is trivial or when the analyst discards both χ_t and υ_t. Exact fiber matching coincides with age matching only on cells with the same verified code and private envelope.

6 The Represented Margin and Market Bridge

In this section, I fix the represented self-transfer margin M, state the benchmark represented-margin bridge, and record the KKT-consistent market factor used by the graph. All objects are local to the maintained margin, current map, and private unit.

Survival-contingent convention. The comparison is per current living person. For

one-step saving margin: (1) start from a current young cell; (2) remove one current resource unit; (3) conditional on survival, deliver represented continuation portfolio over next-period states; (4) survival probabilities enter future leg weights; (5) $\mathcal{Q}$ prices that survival-contingent route; (6) Λ corrects for KKT implementability. Alternative actuarial conventions define different represented margins and ask rebuilding the graph.

6.1 The bridge domain and verified current maps

For cell (t, x), let $P_{t,x}$ be the benchmark continuation law. A *pathwise self-connected perturbation* on M removes one current resource unit at (t, x) and reallocates the compensating future leg only across that individual's represented continuation cells, holding benchmark prices, policies, and constraints fixed. Let $D^{P}_{t,x}$ and $D^{S,M}_{t,x}$ be the private and represented social derivatives.

Assumption 6.1 (Represented domain pathwise derivatives)**.** On M, every (t, x) admits affine pathwise derivatives on admissible self-connected perturbations, with the null perturbation assigned value 0. When the same perturbation is described either pathwise or as the induced cross-sectional perturbation, the two derivatives agree on their common domain.

Definition 6.2 (Nonpaternalism)**.** A criterion is *nonpaternalistic on M* if, for any represented perturbations $\delta, \widetilde{\delta}$ at (t, x), equality of private derivatives implies equality of represented social derivatives, and a strict private ranking implies the same strict represented social ranking. This is the baseline case $\mathfrak{B}(\pi) = 1$. If the planner values the represented future leg more than the individual's private ranking, $\mathfrak{B}(\pi) < 1$; if less, $\mathfrak{B}(\pi) > 1$.

6.2 What the bridge assumes and what it leaves open

The bridge states how the represented continuation enters the planner's valuation and is separate from the map defining current cells. Formally, $\mathfrak{B} : \Pi^{M} \to (0, \infty)$ is a measurable primitive on the declared domain of tuples. It is fixed before the graph is solved, not chosen edge by edge to fit residuals. Three cases fix the convention.

(A) *Private-ranking benchmark.* If the planner uses the individual's private ranking of the represented continuation, then $\mathfrak{B}(\pi) = 1$ and $\mathcal{R}^{S}(\pi) = \mathcal{Q}(\pi)\Lambda(\pi)$.

(B) *Paternalism about continuation.* If the planner values that continuation differently from the individual, then $\mathcal{R}^S(\pi) = \mathcal{Q}(\pi)\Lambda(\pi)\mathfrak{B}(\pi)$. A higher social value corresponds to $\mathfrak{B}(\pi) < 1$; a lower social value corresponds to $\mathfrak{B}(\pi) > 1$.

(C) *Survival, health, or other continuation weights.* Ethical weights on survival, health, or future states enter $\mathfrak{B}$, not χ or υ. They change the edge label, but not current support unless they change the represented margin itself.

Let $\widetilde{\Lambda}(\pi) := \Lambda(\pi)\mathfrak{B}(\pi)$. Positivity makes $\log \mathfrak{B}(\pi)$ well defined. For an exact edge,

$$\log \frac{\eta_t(x_t^{\mathrm{y}})}{\eta_t(x_t^{o})} = \log \mathcal{Q}(\pi) - \log \mathcal{D}^S(\pi) + \log \Lambda(\pi) + \log \mathfrak{B}(\pi). \tag{20}$$

Thus younger residual priority is certified whenever

$$\mathfrak{B}(\pi) > \frac{\mathcal{D}^S(\pi)}{\mathcal{Q}(\pi)\Lambda(\pi)},$$

with the coresponding e^{ε} adjustment under approximate matching. The baseline sets $\mathfrak{B} \equiv 1$. Parametric corrections are primitives; bounded bridge uncertainty is propagated through explicit edge or target-corridor restrictions, and the audit reports how certification changes with the unit, wedge, bridge range, or support.

Consider a finite-life household with state $x = (a, \zeta, w)$, age, nonresource state, and scalar resources. At age a it solves

$$V_a(w, \zeta; m) = \max_{d \in D_a(\zeta, w)} \left\{ u_a(c_a(d, w, \zeta) + m, \zeta) + \beta p_a \int V_{a+1}(W_a(d, w, \zeta, \zeta'), \zeta'; 0) P_a(\zeta, w, d, \mathrm{d}\zeta') \right\} \tag{21}$$

subject to convex constraints

$$g_{aj}(d, w, \zeta) \leq 0, \qquad j = 1, \ldots, J_a. \tag{22}$$

Let $\upsilon_a(w, \zeta) = \partial V_a(w, \zeta; m)/\partial m|_{m=0} > 0$.

Assumption 6.3 (Convex age-structured household class)**.** For each (a, ζ), feasible sets are nonempty and convex, the objective in Equation (21) is concave, and the constraints in Equation (22) satisfy

Slater's condition: relative to the affine constraints, there is a feasible choice that satisfies the inequality constraints strictly. Flow utility is differentiable and strictly concave, $\upsilon_a > 0$, and $w \mapsto \upsilon_a(w, \zeta)$ is continuous and strictly monotone on the support region used for matching. For margin M, the analyst verifies a measurable tuple $\Psi_a^M(\zeta)$ such that equality of (Ψ_a^M, υ_a) identifies the represented future leg, gross market compensation object, and relevant loadings after age alignment.

Remark 6.4 (Constructive certificate for richer state spaces). A primitive certificate lists the represented leg, market price, and KKT loadings, then lets Ψ_a^M be the minimal non-age tuple that identifies them once υ_a and age alignment are fixed.

Definition 6.5 (Verification protocol for the current map)**.** For margin M, define

$$\chi_a^M(w, \zeta) := \Psi_a^M(\zeta), \qquad \Psi_a^M(\zeta) = \min\{\text{non-age primitives identifying } (L^M, \mathcal{Q}^M, \Xi^M, \operatorname{supp} L^M)\}, \tag{23}$$

where the minimum is in the partition-refinement order on the maintained support. On maintained support, a cross-age current match requires

$$\chi_a^M(w, \zeta) = \chi_{a'}^M(\widetilde{w}, \widetilde{\zeta}), \qquad \upsilon_a(w, \zeta) = \upsilon_{a'}(\widetilde{w}, \widetilde{\zeta}).$$

Every strict coarsening requires a separate sufficiency check; refinements remain sufficient and shrink support.

Proposition 6.6 (One-asset saving-margin current map)**.** *In the one-asset life-cycle problem of Section 8, with state $x = (a, b, \varepsilon)$, age-dependent deterministic schedules, age-invariant transition matrix P, monotone private envelope, and represented one-step risk-free saving leg, equality of υ pins down the scalar resource state within a transition-row class. The future-leg law is the survival-contingent row $P_{k\cdot}$, the market object is $1 + r$, the relevant KKT loading is the saving-route borrowing load, and the support is the common one-step continuation support. Hence the verified non-age tuple is the current earnings transition-row type,*

$$\chi_a^M(b, \varepsilon_k) = P_{k\cdot} := (P_{kk'})_{k'}.$$

The full rule also requires equality of υ_a. Distinct rows give current earnings state; coincident rows

give row equivalence classes; further coarsening requires support-specific verification.

Remark 6.7 (Worked one-asset primitive certificate). In the benchmark one-asset model, $\upsilon_a(b, \varepsilon_k) = u'(c_a(b, \varepsilon_k))$. Equality of υ_a recovers the scalar resource state inside a row class, while $P_{k\cdot}$ fixes the non-age continuation composition and support. The KKT-consistent route is represented by $\mathcal{Q}^M = 1 + r$ and $\Lambda^M = [1 - \lambda_a/\upsilon_a]^{-1}$. If regimes or multiple supporting prices change the leg, price, support, or loading, the regime indicator enters Ψ_a^M.

Remark 6.8 (Represented margin dependence and scope). The one-step risk-free saving margin is a benchmark. Risky assets, labor supply, promised utility, or longer legs may enlarge the tuple and require a separate verification.

6.3 KKT-consistent market valuation

Fix an ordered tuple $\pi = (t, x_t^{\mathrm{o}}, x_t^{\mathrm{y}}, x_s^{\mathrm{o}})$, or a finite-support portfolio version of its future leg. Let $\{\delta_R^\pi\}_{R\geq 0}$ remove one current unit at x_t^{y} and add the represented future leg of size R.

Definition 6.9 (Gross market compensation factor)**.** $\mathcal{Q}(\pi)$ is the gross future-leg size that can be supported by one current unit along the represented route. With a supporting state-price density, $\mathcal{Q}(\pi)$ is bounded by the inverse local price and equals it when the leg is locally purchasable.

Definition 6.10 (Represented one-dimensional family and indifference factors)**.** When unique, $\widehat{R}^P(\pi)$ and $\widehat{R}^{S,M}(\pi)$ solve

$$D^P_{t,x_t^{\mathrm{y}}}[\delta^\pi_{\widehat{R}^P(\pi)}] = 0, \qquad D^{S,M}_{t,x_t^{\mathrm{y}}}[\delta^\pi_{\widehat{R}^{S,M}(\pi)}] = 0.$$

Proposition 6.11 (Primitive bridge from represented perturbations to weights)**.** *If the primitive social objective is differentiable and the represented family induces a per-living-person perturbation with density* -1 *on the current cell and density* R *on the represented future portfolio, then*

$$D^{S,M}_{t,x_t^{\mathrm{y}}}[\delta^\pi_R] = -\omega_t(x_t^{\mathrm{y}}) + R\mathcal{V}_s^\omega(\pi), \tag{24}$$

so the represented social indifference factor is

$$\widehat{R}^{S,M}(\pi) = \mathcal{R}^S(\pi) = \frac{\omega_t(x_t^{\mathrm{y}})}{\mathcal{V}_s^\omega(\pi)}. \tag{25}$$

Assumption 6.12 (Represented family bridge regularity)**.** For every exact, approximate, or coarse tuple used below, either Proposition 6.11 applies or the represented family is restricted to a domain satisfying Equations (24) and (25).

Proposition 6.13 (Supporting price/KKT bridge)**.** *Suppose $\mathcal{Q}(\pi)$ is the local marginal exchange rate for the represented leg and the sign-normalized KKT loading of that route is $\Xi(\pi) \in [0, \upsilon_t(x_t^{\mathrm{y}}))$. Then*

$$\widehat{R}^P(\pi) = \mathcal{Q}(\pi) \left[1 - \frac{\Xi(\pi)}{\upsilon_t(x_t^{\mathrm{y}})}\right]^{-1}. \tag{26}$$

The bracketed term is one when all relevant loadings vanish.

Corollary 6.14 (Convex liquid/illiquid extension)**.** *In a convex liquid/illiquid extension with verified supporting prices, the same KKT formula applies after the tuple is augmented by the current illiquid state and relevant adjustment-cost gradients.*

Remark 6.15 (What changes outside the convex class). Nonconvexities can make suporting prices set-valued or introduce regime-specific loadings; then regime indicators may enter the tuple.

Remark 6.16 (Verification checklist for the verified current tuple). For margin M: specify the future leg, derive the market object, list current loadings, collect nonresource primitives in Ψ_a^M, and verify on support that equality of (Ψ_a^M, υ_a) equalizes all margin-relevant objects.

Assumption 6.17 (Local supporting price representation)**.** Every tuple on which the market bridge is invoked has a verified supporting-price/KKT argument yielding $\Xi(\pi) \in [0, \upsilon_t(x_t^{\mathrm{y}}))$ such that

$$\widehat{R}^P(\pi) = \mathcal{Q}(\pi) \left[1 - \frac{\Xi(\pi)}{\upsilon_t(x_t^{\mathrm{y}})}\right]^{-1}. \tag{27}$$

If the perturbation is locally spanned and all relevant constraints are slack, then $\Xi(\pi) = 0$.

Proposition 6.18 (KKT-consistent market bridge)**.** *Suppose Assumptions 3.1, 3.3, 4.1, 6.1, 6.12 and 6.17 hold and the criterion is nonpaternalistic on M. Then every bridge-verified tuple satisfies*

$$\mathcal{R}^S(\pi) = \mathcal{Q}(\pi)\Lambda(\pi), \qquad \Lambda(\pi) = \left[1 - \frac{\Xi(\pi)}{\upsilon_t(x_t^{\mathrm{y}})}\right]^{-1} \geq 1, \tag{28}$$

so $\mathcal{R}^S(\pi) \geq \mathcal{Q}(\pi)$ in the baseline $\mathfrak{B} \equiv 1$ case. Equality holds whenever $\Xi(\pi) = 0$; a sufficient primitive

condition is local spanning and local slackness. With a bridge correction, define $\widetilde{\Lambda}(\pi) = \Lambda(\pi)\mathfrak{B}(\pi)$ *and replace the right side by* $\mathcal{Q}(\pi)\widetilde{\Lambda}(\pi)$.

Remark 6.19 (Economic meaning of the wedge). $\Lambda(\pi)$ is the inverse share of the current private envelope derivative available for the future leg after KKT loadings are netted out. If $\mathcal{D}^S(\pi) = \mathcal{Q}(\pi)$, then Propositions 5.5 and 6.18 give $\eta_t(x_t^{\mathrm{y}})/\eta_t(x_t^{\mathrm{o}}) = \Lambda(\pi)$.

Proposition 6.20 (PVEU-balanced target comparisons reduce to target averages)**.** *Fix a represented financing rule and write two local policy perturbations in* PVEU *units as* $\Delta^A = \tau^A - \phi$ *and* $\Delta^B = \tau^B - \phi$*, with common financing measure* ϕ*. If both are admissible and* PVEU*-integrable, then*

$$D\mathcal{W}[\Delta^A] - D\mathcal{W}[\Delta^B] = \int \eta_t(x)(\tau^A - \tau^B)(\mathrm{d}x). \tag{29}$$

If $\tau^A(\mathcal{X}) = \tau^B(\mathcal{X}) > 0$*, the sign equals the sign of the difference in* η*-weighted target averages.*

Remark 6.21 (Policy to margin mapping). A full policy maps into this local object only after specifying the represented financing rule, private unit, support, and component anchors. The quantitative section reports the supported local target object and explicit omitted-support layers.

Corollary 6.22 (State-price form of the restriction)**.** *If the represented leg is locally purchasable at state-price density* $q_{t,s}$*, then* $\mathcal{R}^S(\pi) = q_{t,s}(x_s^{\mathrm{o}} \mid x_t^{\mathrm{y}})^{-1}\Lambda(\pi)$ *in the singleton case, with the analogous portfolio price for finite-support legs.*

7 Supported Graphs and Rationalizability

Exact fiber matching and the market bridge imply a restriction on residual priority. Given the margin, map, private unit, bridge, and support, discounting below market compensation requires greater residual priority for the younger cell on populated exact fibers. Once the current-cell graph is constructed, rationalizability is a standard potential problem, familiar from revealed-preference and convex-analysis arguments (Afriat, 1967; Rockafellar, 1970; Varian, 1982). What is nonstandard is the step that precedes it: mapping the economic environment into vertices, labels, support, units, and anchors.

Proposition 7.1 (Residual priority restriction under a verified comparison system)**.** *Let* $\pi = (t, x_t^{\mathrm{o}}, x_t^{\mathrm{y}}, x_s^{\mathrm{o}})$ *be a bridge-verified comparison tuple: an exact-fiber comparison tuple for which the represented family, supporting-price and Karush-Kuhn-Tucker (KKT) representation, and represented-domain bridge are verified. Suppose Assumptions 3.1, 3.3, 4.1, 6.1, 6.12 and 6.17 hold and the criterion is nonpaternalistic on the represented domain* M*. Then*

$$\log \frac{\eta_t(x_t^{\mathrm{y}})}{\eta_t(x_t^{\mathrm{o}})} = \log \mathcal{Q}(\pi) - \log \mathcal{D}^S(\pi) + \log \Lambda(\pi) \geq \log \mathcal{Q}(\pi) - \log \mathcal{D}^S(\pi). \tag{30}$$

Thus, if

$$\mathcal{D}^S(\pi) < \mathcal{Q}(\pi), \tag{31}$$

then

$$\eta_t(x_t^{\mathrm{y}}) > \eta_t(x_t^{\mathrm{o}}). \tag{32}$$

Conditional residual age neutrality fails on any fiber that supports such a tuple. If $\mathcal{D}^S(\pi) = \mathcal{Q}(\pi)$*, then*

$$\frac{\eta_t(x_t^{\mathrm{y}})}{\eta_t(x_t^{\mathrm{o}})} = \Lambda(\pi),$$

so any residual younger tilt is exactly wedge-driven.

Remark 7.2 (Scope of the nonpaternalistic benchmark). With a bridge correction, set $\widetilde{\Lambda}(\pi) := \Lambda(\pi)\mathfrak{B}(\pi)$. Then Equation (30) becomes $\log(\eta_t(x_t^{\mathrm{y}})/\eta_t(x_t^{\mathrm{o}})) = \log \mathcal{Q}(\pi) - \log \mathcal{D}^S(\pi) + \log \widetilde{\Lambda}(\pi)$, and the younger tilt conclusion requires $\mathcal{D}^S(\pi) < \mathcal{Q}(\pi)\widetilde{\Lambda}(\pi)$. The baseline maintained in the numerical audit is $\mathfrak{B} \equiv 1$.

7.1 Exact comparison graphs and the rationalizability theorem

Definition 7.3 (Exact fiber current comparison graph)**.** Fix date t and a represented margin. The exact fiber current comparison graph $G_t = (V_t, E_t)$ has vertices equal to current date-t cells that belong to a populated exact fiber supporting an admissible comparison tuple. A directed edge $e = (x^{\mathrm{y}}, x^{\mathrm{o}})$ belongs to E_t if $a(x^{\mathrm{o}}) > a(x^{\mathrm{y}})$, the two cells lie in the same exact fiber, and some witness leg $x_s^{\mathrm{o}} \in \Gamma_{t,s}(x^{\mathrm{y}})$ reaches age $a(x^{\mathrm{o}})$.

The graph is current-cell based. Future legs label edges. Exact fibers are the conceptual

benchmark. Finite applications use approximate graphs with explicit private-envelope bands.

Proposition 7.4 (Exact edge weights)**.** *For an edge $e = (x^{\mathrm{y}}, x^{\mathrm{o}})$ and witness x_s^{o}, write*

$$\pi(e; x_s^{\mathrm{o}}) := (t, x^{\mathrm{o}}, x^{\mathrm{y}}, x_s^{\mathrm{o}})$$

and define the corrected bridge wedge $\widetilde{\Lambda}(\pi) := \Lambda(\pi)\mathfrak{B}(\pi)$, with $\mathfrak{B} \equiv 1$ in the baseline. The edge label is

$$g_t(e; x_s^{\mathrm{o}}) := \log \mathcal{Q}(\pi(e; x_s^{\mathrm{o}})) - \log \mathcal{D}^S(\pi(e; x_s^{\mathrm{o}})) + \log \widetilde{\Lambda}(\pi(e; x_s^{\mathrm{o}})). \tag{33}$$

Under the assumptions of Proposition 7.1 in the baseline, and under those assumptions plus the corrected bridge relation $\mathcal{R}^S = \mathcal{Q}\Lambda\mathfrak{B}$ when $\mathfrak{B} \neq 1$,

$$g_t(e; x_s^{\mathrm{o}}) = \log \eta_t(x^{\mathrm{y}}) - \log \eta_t(x^{\mathrm{o}}). \tag{34}$$

Hence the weight is independent of the witness; write it as $g_t(e)$.

Theorem 7.5 (Current-graph rationalizability of imposed local discount labels)**.** *Fix a represented margin M, current map χ, private unit υ, and bridge domain. Construct the finite exact current-date comparison graph from that triplet. For each directed current edge $e = (x^{\mathrm{y}}, x^{\mathrm{o}})$, let Π_e be the set of bridge-verified witness tuples $\pi = (t, x^{\mathrm{o}}, x^{\mathrm{y}}, x_s^{\mathrm{o}})$. Let $\widetilde{\Lambda}(\pi) = \Lambda(\pi)\mathfrak{B}(\pi)$ denote the corrected bridge wedge, with $\mathfrak{B} \equiv 1$ in the baseline. An imposed local schedule $\bar{\mathcal{D}}^S$ is rationalizable on this supported current graph by positive residual multipliers if and only if there are edge labels*

$$\bar{g}(e) = \log \mathcal{Q}(\pi) - \log \bar{\mathcal{D}}^S(\pi) + \log \widetilde{\Lambda}(\pi), \qquad \pi \in \Pi_e,$$

that satisfy two restrictions. First, all witness labels attached to the same current edge agree (parallel-witness consistency). Second, every closed walk in the underlying undirected graph has zero signed $\bar{g}$ sum, counting reverse traversal with the opposite sign (cycle consistency). When these restrictions hold, there exists $\widetilde{\eta} > 0$ such that

$$\log \widetilde{\eta}(x^{\mathrm{y}}) - \log \widetilde{\eta}(x^{\mathrm{o}}) = \bar{g}(e)$$

for every edge. The solution is unique up to one multiplicative constant per connected component. Relative residual-multiplier levels across disconnected components are not identified without additional anchors. If targets load differently across disconnected components, target comparisons are not identified without component anchors. Countable or measurable graphs are treated componentwise under integrable, path-independent sums.

Proposition 7.6 (Endogenous exact edge weights are potentials)**.** *For a directed exact edge chain $c = (x^0, x^1, \dots, x^n)$ in G_t, define*

$$G_t(c) := \sum_{\ell=1}^{n} g_t(x^{\ell-1}, x^{\ell}). \tag{35}$$

Under the assumptions of Proposition 7.1,

$$G_t(c) = \log \eta_t(x^0) - \log \eta_t(x^n). \tag{36}$$

Consequently: (i) two directed exact edge chains with the same endpoints have the same total weight; (ii) every closed walk in the symmetrized graph has zero signed total weight; and (iii) on each connected component C of the symmetrized graph there is a potential $\phi_t^C : C \to \mathbb{R}$, unique up to an additive constant, such that

$$g_t(x^{\mathrm{y}}, x^{\mathrm{o}}) = \phi_t^C(x^{\mathrm{y}}) - \phi_t^C(x^{\mathrm{o}})$$

for every directed edge in C. One choice is $\phi_t^C = \log \eta_t|_C$.

Corollary 7.7 (Component normalization and recursion)**.** *Fix a connected component C and anchor $x^\star \in C$. Once $\eta_t(x^\star) > 0$ is fixed, every within component ratio is uniquely determined by exact edge weights. Any exact edge spanning tree enforcing*

$$\eta_t(x^{\mathrm{y}}) = \exp(g_t(x^{\mathrm{y}}, x^{\mathrm{o}}))\eta_t(x^{\mathrm{o}})$$

on tree edges gives the same ratios. Multiplying the anchor by a common positive constant rescales the component and changes no ratio.

Remark 7.8 (Outer component envelope)*.* Disconnected components leave relative constants unidentified. A conservative current-goods closure sets $\bar{m} := \log(\max_{x \in S} \upsilon_t(x) / \min_{x \in S} \upsilon_t(x))$, the main-

tained support range of private current-goods marginal values. This is not cross-component identification; it is an outer bound on the missing exchange rate. If $[\underline{\Delta}, \overline{\Delta}]$ is a fixed-anchor interval, $[\underline{\Delta} - \bar{m}, \overline{\Delta} + \bar{m}]$ is the component-envelope interval.

Remark 7.9 (What the graph structure adds). The graph converts pairwise restrictions into componentwise recursions and exposes disconnected support and anchor dependence. Nonzero cycle residuals diagnose imposed or operational finite-grid edge weights, such as fixed nearest-neighbor correspondences or external schedules. Endogenous exact edge weights telescope as a gradient. The object is local to the current-date graph. A globally consistent dated welfare-weight system would require an enlarged space-time graph that also identifies every dated future leg with its appearances as a current vertex in other graphs.

Corollary 7.10 (Approximate pairwise band)**.** *Let $\bar{\pi} = (t, x_t^{\mathrm{o}}, x_t^{\mathrm{y}}, x_s^{\mathrm{o}})$ be an admissible bridge-verified ordered tuple in the sense of Definition 5.2, with $s = t + a(x_t^{\mathrm{o}}) - a(x_t^{\mathrm{y}})$, $a(x_t^{\mathrm{o}}) > a(x_t^{\mathrm{y}})$, $\chi_t(x_t^{\mathrm{o}}) = \chi_t(x_t^{\mathrm{y}})$, $x_s^{\mathrm{o}} \in \Gamma_{t,s}(x_t^{\mathrm{y}})$, and*

$$|\log \upsilon_t(x_t^{\mathrm{o}}) - \log \upsilon_t(x_t^{\mathrm{y}})| \le \varepsilon.$$

Under the assumptions of Proposition 7.1,

$$\left| \log \frac{\eta_t(x_t^{\mathrm{y}})}{\eta_t(x_t^{\mathrm{o}})} - \left[\log \mathcal{Q}(\bar{\pi}) - \log \mathcal{D}^S(\bar{\pi}) + \log \widetilde{\Lambda}(\bar{\pi}) \right] \right| \le \varepsilon. \tag{37}$$

Equivalently,

$$\log \frac{\eta_t(x_t^{\mathrm{y}})}{\eta_t(x_t^{\mathrm{o}})} \in \left[\log \mathcal{Q}(\bar{\pi}) - \log \mathcal{D}^S(\bar{\pi}) + \log \widetilde{\Lambda}(\bar{\pi}) - \varepsilon,\ \log \mathcal{Q}(\bar{\pi}) - \log \mathcal{D}^S(\bar{\pi}) + \log \widetilde{\Lambda}(\bar{\pi}) + \varepsilon \right]. \tag{38}$$

If

$$\mathcal{D}^S(\bar{\pi}) < \mathcal{Q}(\bar{\pi}) \widetilde{\Lambda}(\bar{\pi}) e^{-\varepsilon}, \tag{39}$$

then $\eta_t(x_t^{\mathrm{y}}) > \eta_t(x_t^{\mathrm{o}})$. In the baseline $\mathfrak{B} \equiv 1$, $\Lambda \ge 1$, so the wedge-free sufficient condition $\mathcal{D}^S(\bar{\pi}) < \mathcal{Q}(\bar{\pi}) e^{-\varepsilon}$ also certifies younger tilt. Certifying the opposite sign from this approximate band requires $\mathcal{D}^S(\bar{\pi}) > \mathcal{Q}(\bar{\pi}) \widetilde{\Lambda}(\bar{\pi}) e^{\varepsilon}$.

Proposition 7.11 (Approximate chain identity and endpoint mismatch)**.** *Fix date t and a directed*

current cell chain $c = (x^0, x^1, \dots, x^n)$. For each edge ℓ, suppose there is a bridge-verified admissible approximate tuple

$$\bar{\pi}_\ell = (t, x^\ell, x^{\ell-1}, x^{\mathrm{o}}_{s_\ell})$$

with maintained current map equality, witness $x^{\mathrm{o}}_{s_\ell} \in \Gamma_{t,s_\ell}(x^{\ell-1})$, and mismatch

$$\varepsilon_\ell := |\log \upsilon_t(x^\ell) - \log \upsilon_t(x^{\ell-1})|.$$

Define

$$\widetilde{g}^\ell_t := \log \mathcal{Q}(\bar{\pi}_\ell) - \log \mathcal{D}^S(\bar{\pi}_\ell) + \log \widetilde{\Lambda}(\bar{\pi}_\ell) \tag{40}$$

and

$$\widetilde{G}_t(c) := \sum_{\ell=1}^{n} \widetilde{g}^\ell_t. \tag{41}$$

Under the assumptions of Proposition 7.1,

$$\widetilde{G}_t(c) = \log \omega_t(x^0) - \log \omega_t(x^n). \tag{42}$$

Hence any second approximate chain $\widetilde{c}$ with the same endpoints satisfies

$$\widetilde{G}_t(c) = \widetilde{G}_t(\widetilde{c}). \tag{43}$$

Moreover,

$$\widetilde{G}_t(c) - (\log \eta_t(x^0) - \log \eta_t(x^n)) = \log \upsilon_t(x^0) - \log \upsilon_t(x^n), \tag{44}$$

so

$$\left|\widetilde{G}_t(c) - (\log \eta_t(x^0) - \log \eta_t(x^n))\right| \le \sum_{\ell=1}^{n} \varepsilon_\ell. \tag{45}$$

If each edge has mismatch at most $\bar{\varepsilon}$, the endpoint mismatch is at most $n\bar{\varepsilon}$.

Proposition 7.12 (Finite-grid approximate-graph convergence)**.** *Let G^0 be an exact-fiber graph on a compact supported domain with finitely many connected components after the stated component anchors. Let G_n be finite approximate graphs generated from partitions with mesh $h_n \downarrow 0$ and matching tolerances $\varepsilon_n \downarrow 0$. Suppose: (i) every exact edge and target cell has approximating finite-*

grid counterparts; (ii) no sequence of approximate edges converges outside the exact edge relation; (iii) the composite edge label $\log \mathcal{Q} - \log \bar{\mathcal{D}}^S + \log \widetilde{\Lambda}$ *and the target weights are continuous on the supported domain; (iv) the normalized feasible sets for the finite programs are uniformly bounded after component anchoring; and (v) the anchored finite feasible sets are nonempty for all sufficiently large* n *and converge inner semicontinuously to the exact anchored set. Embed each finite potential as the partition-cell piecewise-constant function on the exact supported domain, with anchored components identified in* L^∞ *modulo null sets. Then the feasible potential sets converge in Hausdorff distance in this common metric space to the exact anchored feasible set, and the identified target interval in Equation* (51) *satisfies*

$$\underline{\Delta}_{AB}^{(n)} \to \underline{\Delta}_{AB}^{0}, \qquad \overline{\Delta}_{AB}^{(n)} \to \overline{\Delta}_{AB}^{0}.$$

Thus shrinking the resource grid and matching tolerance recovers the exact-fiber interval when support and component structure are stable. In KKT environments the regime code is explicit: borrowing-kink cells are either retained as boundary cells or removed in a separate support audit, not treated as smooth interiors.

Remark 7.13 (From exact potential to finite-grid recursion). The exact theorem gives a $\log \eta$ potential. Approximate chain totals telescope in raw welfare weights; endpoint private-scale mismatch controls their distance from the residual multiplier potential.

Remark 7.14 (From tuplewise to class level restrictions). Pairwise ε bounds become class-level bounds with regularity of a declared class summary of η_t across nearby private envelopes. Here $\bar{\eta}_t(u, e^z)$ denotes a maintained positive measurable selection, average, or envelope over $\{x : \chi_t(x) = u,\ \upsilon_t(x) = e^z\}$; if $z \mapsto \log \bar{\eta}_t(u, e^z)$ is L-Lipschitz, moving ε in $z = \log \upsilon_t$ adds at most $L\varepsilon$. For multidimensional states, a declared metric d on sufficient codes yields a relaxed edge when $d(x, x') \le \delta$, with graph band $\varepsilon_e + L\delta$; exact matching is $\delta = 0$.

The restriction is local to represented margins and to the current comparison graph. It reveals residual multiplier differences under the maintained map, unit, and bridge. Global policy rankings, space-time consistency of dated future legs, independent age ethics, and behavioral environments outside private ranking require extra structure.

Set $\Psi_t(x) := (\chi_t(x), \upsilon_t(x))$, $\nu_t := \Psi_{t\#}\mu_t$, and let $\{\mu_{t,g}\}_g$ be the regular conditional law. An

exact fiber comparison system is a measurable subprobability kernel $K_t(g, \mathrm{d}\pi)$ over admissible bridge-verified exact fiber tuples whose normalized current marginals are absolutely continuous with respect to $\mu_{t,g}$ on fibers with $K_t(g, \Pi) > 0$; unsupported fibers receive zero mass. It induces

$$\Theta_t(\mathrm{d}\pi) := \int K_t(g, \mathrm{d}\pi)\, \nu_t(\mathrm{d}g).$$

Note that almost-everywhere and positive-measure statements below are with respect to Θ_t. This prevents the comparison system from concentrating on representatives outside the full measure versions used for conditional residual neutrality.

Corollary 7.15 (Three way tension)**.** *Fix such a system with induced tuple measure Θ_t. The following three statements cannot all hold:*

(i) $\mathcal{D}^S(\pi) \leq \mathcal{Q}(\pi)$ *for almost every admissible bridge-verified tuple, with strict inequality on a positive measure set;*

(ii) the social criterion is nonpaternalistic; and

(iii) the social criterion is conditionally residual age neutral on every relevant comparison fiber.

Moreover, (ii) and (iii) imply

$$\mathcal{D}^S(\pi) = \mathcal{Q}(\pi)\Lambda(\pi) \geq \mathcal{Q}(\pi)$$

for almost every bridge-verified tuple in the system.

8 A Quantitative Certification Audit

This section audits the theory as a local diagnostic. Policy rankings require additional support, unit, completion, and anchor assumptions. The maintained triplet is the represented one-step saving margin M, the verified current-cell map χ, and the current-goods private unit $v = u'(c)$. Each number is conditional on that triplet unless a row explicitly rebuilds the graph under another maintained object. The output is a certification frontier: the table reports which sign claims are certified under which support, unit, wedge, and anchor conventions.

8.1 One-asset benchmark and KKT-consistent bridge

The analytical benchmark is a finite-life one-asset economy with uninsurable labor income risk and a borrowing limit, following Huggett (1993), Aiyagari (1994), and Conesa and Krueger (1999). With $x = (a, b, \varepsilon)$, households solve

$$V_a(b, \varepsilon; m) = \max_{b' \geq \underline{b}_a} \{u(c + m) + \beta p_a \, \mathbb{E}[V_{a+1}(b', \varepsilon'; 0) \mid \varepsilon]\}, \qquad c + b' = y_a(\varepsilon) + (1 + r)b, \tag{46}$$

with terminal condition $V_A(b, \varepsilon; m) = u(c_A + m)$. For the calibration, I use Conesa and Krueger (1999) for demographics and earnings, Gourinchas and Parker (2002) for preferences and the interest rate, and Arias et al. (2023) for survival: entry age 20, retirement age 65, terminal age 85, population growth 1.1 percent, $\beta = 0.9569$, $\sigma = 1.3969$, $r = 0.0344$, replacement ratio 0.5, no unsecured debt, an 800-point curved asset grid, and earnings states $(0.73, 1.27)$ with rows $(0.82, 0.18)$ and $(0.18, 0.82)$. The represented leg is one-step survival-contingent risk-free saving.

Proposition 8.1 (Risk-free saving specialization and KKT-consistent Euler wedge)**.** *In Equation* (46)*, fix younger cell* (a, b_i, ε_k)*, let* $g_a(i, k)$ *be the chosen next asset index, and let* $m_a(i, k)$ *be the direct* $\log \upsilon$ *matched older asset index. On the one-step risk-free portfolio that removes one current unit and adds the same next-period unit in each survival-contingent continuation earnings state at asset* $b_{g_a(i,k)}$*, Assumption 6.17 holds with*

$$\mathcal{Q}_a^{(i,k)} = 1 + r \tag{47}$$

and

$$\Lambda_a^{(i,k)} = \frac{u'(c_a(b_i, \varepsilon_k))}{\beta p_a (1 + r) \sum_{k'} P_{kk'} u'(c_{a+1}(b_{g_a(i,k)}, \varepsilon_{k'}))} \geq 1. \tag{48}$$

For the labeled one-step tuple π_{aik} *used by the edge,*

$$\frac{\eta_a(b_i, \varepsilon_k)}{\eta_{a+1}(b_{m_a(i,k)}, \varepsilon_k)} = \frac{1 + r}{\mathcal{D}^S(\pi_{aik})} \Lambda_a^{(i,k)} \frac{\upsilon_{a+1}(b_{m_a(i,k)}, \varepsilon_k)}{\upsilon_a(b_i, \varepsilon_k)}. \tag{49}$$

The final ratio equals one under exact matching and lies in $[e^{-\varepsilon}, e^{\varepsilon}]$ *under tolerance radius* ε*. Replacing endogenous tuple ratios by an imposed age schedule* $\bar{\mathcal{D}}_a^S$ *turns Equation* (49) *into the graph restriction tested below.*

Endogenous tuple-specific $\mathcal{D}^S(\pi)$ is an identity. An imposed $\bar{\mathcal{D}}_a^S$ is a restriction. Unless stated otherwise, diagnostics use the market benchmark $\bar{\rho}^S = r$ and the one-step survival-contingent risk-free witness leg. The verified current-cell map is transition-row type, equal here to current earnings state. The symbol $g_a(i,k)$ defines the represented continuation leg from the grid policy; the maintained wedge is the KKT-consistent projection, not the raw finite-grid Euler residual. One-step overlap is essentially complete in the two-state benchmark: overall and minimum age-specific overlap are 1.000000, and younger mass-weighted mean log mismatch is 4.40×10^{-4}. The current-map verification solves the household problem, computes $\upsilon = u'(c)$, records the transition row and KKT loading for the represented saving margin, and reports overlap, mismatch, and dispersion diagnostics before target statistics are computed. In the five-state tolerance graph, $\max|\Delta \log Q| = 0.00000$, the transition-row mismatch share is 0.0000, and the mean and 95th percentile of $|\Delta \log \Lambda|$ are 0.00092 and 0.00649; the replication output also records boundary-regime and adjacent-monotonicity flags.

8.2 Main five-state diagnostic calibration and finite graph program

The main diagnostic calibration is the five-state hump block. It keeps preferences, ages, survival, borrowing limit, and interest rate, uses a 450-point asset grid, adds hump-shaped deterministic earnings, and uses a five-state Rouwenhorst process with levels $(0.564, 0.738, 0.965, 1.261, 1.649)$ and persistence 0.82. The central current-earnings row used in the focal target belongs to this block. A warm-up statistic with target A at ages 20 to 29 and target B at ages 40 to 49 in the central current-earnings row has verified-map overlap 0.7145 and interval $[0.00090, 0.01444]$ under the stated tolerance protocol. Age matching raises overlap to 0.9673 and widens the interval to $[-0.02605, 1.19061]$. Support gains therefore come with contamination and weaker graph discipline.

Let I be the full retained graph vertex set on the supported comparison domain; target weights may be 0 on connector vertices that enter only through edge constraints. Let E_ε be the maintained tolerance edge set. An edge is retained when the non-age code matches and the private-unit mismatch is within its stated tolerance. The search cap K is a computational cap used to find all retained candidates inside the tolerance set. For edge $e = (y, o)$, let $H_e := \log \mathcal{Q}(e) - \log \bar{\mathcal{D}}^S(e) + \log \widetilde{\Lambda}(e)$ and mismatch radius ε_e. The baseline audit sets $\mathfrak{B} \equiv 1$, so $\widetilde{\Lambda} = \Lambda$; Table 6 also reports a bounded bridge-correction corridor. With one anchor i_C in each connected component, feasible log multipliers

are

$$\mathcal{Z}_\varepsilon := \{z \in \mathbb{R}^I : z_{i_C} = 0 \text{ for all } C, \quad H_e - \varepsilon_e \le z_y - z_o \le H_e + \varepsilon_e \text{ for all } e \in E_\varepsilon\}. \tag{50}$$

For target mass vectors w^A, w^B on the supported domain,

$$\Delta_{AB}(z) := \log \frac{\sum_i w_i^A e^{z_i}}{\sum_i w_i^A} - \log \frac{\sum_i w_i^B e^{z_i}}{\sum_i w_i^B}, \qquad [\underline{\Delta}_{AB}, \overline{\Delta}_{AB}] = \left[\inf_{z \in \mathcal{Z}_\varepsilon} \Delta_{AB}(z), \sup_{z \in \mathcal{Z}_\varepsilon} \Delta_{AB}(z)\right]. \tag{51}$$

The finite-graph interval is a tolerance-specific maintained object. Point summaries are deterministic summaries. Cycle or parallel-label residuals are rationalizability failures.

If component constants c_C are left free after solving within-component potentials $\tilde{z}$, then

$$\Delta_{AB}(c) = \log \frac{\sum_C e^{c_C} A_C}{\sum_i w_i^A} - \log \frac{\sum_C e^{c_C} B_C}{\sum_i w_i^B}, \quad A_C = \sum_{i \in C} w_i^A e^{\tilde{z}_i}, \quad B_C = \sum_{i \in C} w_i^B e^{\tilde{z}_i}. \tag{52}$$

Targets that load differently across disconnected components require a component-anchor exposure report. A bounded-anchor sensitivity set replaces unrestricted c_C with $c_C \in [-\bar{c}, \bar{c}]$. Increasing $\bar{c}$ traces the minimum anchor restriction needed for sign certification. In the focal audit, sign certification is lost once $\bar{c} = 0.00333$ log points, about 0.33 percent log points. The unrestricted-anchor row is the limiting case and is unidentified when unrounded target mass lies in components not shared by the other target.

Table 3: Certification frontier for the focal target comparison

Maintained system	Support	Unit	Anchors	Wedge	Certified sign?	Interval
Age-only	full	implicit dollars	none	none	No	[-0.04044, 0.15093]
Age-only	common	implicit dollars	none	none	No	[-0.00967, 0.07886]
Verified cell	common	current goods	fixed	KKT	Yes, conditional	[-0.00819, -0.00298]
Verified cell	common	current goods	free	KKT	No	$[-\infty, +\infty]$
Verified cell	common	current goods	outer	KKT	No	[-2.16877, 2.15760]
Largest common component	common comp.	current goods	within comp.	KKT	Yes, within comp.	[0.00004, 0.00082]
Unit-rescaled graph	rebuilt	age-state	fixed	KKT	No	[-0.48701, 0.50273]
Richer-state system	rebuilt	current goods	fixed	KKT	No	[-0.03237, 0.06770]

Notes. Intervals are supported normalized residual-multiplier contrasts; positive Δ_{AB} favors target A. Certified means sign-certified under the maintained row. Free anchors are unbounded. The outer-envelope row restricts component gaps by the global private marginal-utility log range on maintained support.

The focal target comparison has no unconditional sign. The negative interval is certified only under fixed component anchors and the current-goods unit. Free anchors leave the normalized

contrast unidentified, while the largest common component gives the opposite local sign. The fixed-anchor negative interval comes from cross-component normalization and asymmetric target exposure, not from any contradiction with edgewise younger tilt.

Table 4: Discount-schedule frontier for the focal target comparison

Candidate annual ρ^S	Fixed-anchor interval	Free-anchor status	Largest-component interval	Conditional fixed-anchor sign	Free-anchor sign?
0.00%	[0.65797, 0.66309]	Unidentified	[0.66200, 0.66254]	positive	No
2.00%	[0.26804, 0.27311]	Unidentified	[0.27570, 0.27621]	positive	No
3.00%	[0.07594, 0.08098]	Unidentified	[0.08540, 0.08588]	positive	No
3.44%	[−0.00819, −0.00298]	Unidentified	[0.00004, 0.00082]	negative	No
4.00%	[−0.11429, −0.10928]	Unidentified	[−0.10307, −0.10261]	negative	No

Notes. The table varies the imposed local social discount schedule holding the calibration, target pair, represented margin, and current-goods unit fixed. The market benchmark is $\rho^S = r = 3.44\%$. With unrestricted component anchors every reported sign is unidentified.

8.3 Local target comparison on common support

Incomplete overlap separates the supported PVEU comparison on the represented margin from a full policy ranking in physical resource units. The target pair is a focused diagnostic: it asks whether an age sign survives once young and old cells are compared under the same current state and private unit.

Proposition 8.2 (What common-support target comparisons identify)**.** *Fix two local* PVEU*-target perturbations satisfying Proposition 6.20, and let $S \subseteq \mathcal{X}$ be any maintained support set. Then*

$$D\mathcal{W}[\Delta^A] - D\mathcal{W}[\Delta^B] = \int_S \eta_t(x)(\tau^A - \tau^B)(\mathrm{d}x) + \int_{S^c} \eta_t(x)(\tau^A - \tau^B)(\mathrm{d}x). \tag{53}$$

A common-support comparison identifies the level first term conditional on the maintained supported weighting system, including component anchors and point-summary choices. The reported Δ_{AB} is a supported normalized residual-multiplier contrast on S; when retained masses differ, it need not equal the unnormalized level contribution in sign or scale. If $\eta_t(x) \in [\underline{\eta}, \overline{\eta}]$ on S^c for $(\tau^A + \tau^B)$ almost everywhere x, the omitted term lies in

$$\left[\underline{\eta}\,\tau^A(S^c) - \overline{\eta}\,\tau^B(S^c),\ \overline{\eta}\,\tau^A(S^c) - \underline{\eta}\,\tau^B(S^c)\right]. \tag{54}$$

Support and within-support rematching both matter. Target A puts equal mass on ages 25 to

34 in the central current earnings row. Target B puts equal mass on ages 45 to 54 on the same represented margin. Age matching gives $\Delta_{AB} = 0.01292$ on full support and 0.00697 on common support. On that same domain and under fixed component anchors, verified current-cell weights give $\Delta_{AB} = -0.00481$ with diagnostic interval $[-0.00819, -0.00298]$. The -0.01773 log-point shift from age-based full support to verified current-cell common support decomposes into -0.00595 from support exclusion and -0.01178 from within-support rematching. Common support retains 0.3706 of target A mass and 0.9338 of target B mass.

The component exposure is the main vulnerability and diagnostic lesson. The maintained graph has 72,171 vertices, 249,501 edges, 3,737 components, and 181,067 independent cycles; target mass largely lies in cyclic components. Target A is concentrated in one component, target B is dispersed, and unrestricted anchors make the comparison unbounded. The current-goods outer envelope in Remark 7.8 uses global private marginal-utility log range 2.16058 and gives $[-2.16877, 2.15760]$: finite, explicit, and too wide to certify a sign. Fixed-anchor and largest-component rows are conditional local comparisons, not cross-component identification.

Table 5: Component exposure for the focal target pair

Component exposure statistic	Target A	Target B
Mass in components shared with the other target	1.0000	0.2797
Component Herfindahl index	0.9999	0.1742
Mass in largest common component	0.3706	0.2612

Notes. The first row is normalized by each target's graph-supported mass; the Herfindahl index uses retained component shares. The largest-common-component row is normalized by original target mass. The unrounded target-A shared share is 0.99996, so a small A-only mass remains.

8.4 Omitted support, unit rebuilds, and KKT-consistent wedges

Table 6 treats the private unit, bridge, and wedge as identification primitives. The supported comparison leaves omitted support, unit/bridge, and wedge implementation layers; support shares are over the focal target domain. The current-goods unit is tied to the planner's physical resource constraint, while the age-state rescaled unit rebuilds support, candidates, components, and intervals through $\widetilde{v}^{(\theta)} = v/\bar{v}_a(k)^\theta$. The baseline sign is certified for $\theta \leq 0.50$ and bridge corridor $|\Delta \log \mathfrak{B}| \leq 0.001$, but not by $\theta = 0.75$ or $\theta = 1$.

My raw-Euler row is a numerical stress test. It shows what happens if finite-grid Euler residuals are propagated as economic wedges. The maintained object uses the KKT-consistent projection: set $\widehat{\lambda}_a = \max\{u'(c_a) - E_a, 0\}$ on boundary cells and 0 on strict interiors up to tolerance, and use $\Lambda = [1 - \widehat{\lambda}/u'(c)]^{-1}$ clipped at one before graph recursion. On the baseline margin, strict interior cells carry 0.8440 of positive mass and boundary-loading cells 0.1560. The implemented wedge mean and 95th percentile are 1.0119 and 1.0839.

Table 6: Unit path, omitted support, and wedge diagnostics

Specification	θ	Graph rule	Target support share	Components	Point	Interval or bound	Certification
Current-goods unit	0.00	tolerance graph	0.7472	3737	-0.00481	[-0.00819, -0.00298]	negative
Bounded bridge, $\bar{b} = 0.001$	none	fixed graph corridor	0.7472	3737	-0.00481	[-0.00919, -0.00198]	negative
Unit path, $\theta = 0.25$	0.25	rebuilt tolerance graph	0.7573	62	-0.00457	[-0.01611, -0.00281]	negative
Unit path, $\theta = 0.50$	0.50	rebuilt tolerance graph	0.7888	62	-0.02694	[-0.08342, -0.02136]	negative
Unit path, $\theta = 0.75$	0.75	rebuilt tolerance graph	0.8166	47	-0.03167	[-0.28857, 0.30268]	no
Age-state rescaled unit	1.00	rebuilt tolerance graph	0.9895	37	0.04076	[-0.48701, 0.50273]	no
Direct raw Euler proxy wedge	none	diagnostic five-nearest graph	0.7472	77	0.03032	[-0.97832, 0.98022]	no
Illustrative lower-tail completion	none	completion bound	1.0000	not applicable	not applicable	[-0.02902, -0.02402]	maintained completion

Notes. Target support share is over focal target mass; candidate share in Table 7 is over tolerance candidates. The bridge row reports the induced target-average corridor $|\Delta \log \mathfrak{B}| \leq 0.001$ on the fixed graph; the fixed-anchor sign is lost only when this corridor reaches 0.00298. Unit-path rows rebuild the graph. The raw Euler proxy uses a diagnostic five-nearest graph and unprojected finite-grid Euler residuals.

8.5 Locality, grid discipline, and richer states

Table 7 reports grid refinement and tolerance-first matching. Its candidate support share is computed over the tolerance-candidate graph, and not over the focal target domain in Table 6; note also that each tolerance row is a maintained finite-graph estimand, not by itself a joint proof of exact-fiber convergence. Grid mismatch is small. The maintained tolerance row uses $\varepsilon = 0.005$ and an exhaustive search cap $K = 58$. Holding targets fixed, higher curvature $\sigma = 2$ gives -0.00444 with $[-0.00607, -0.00348]$ and $\beta = 0.97$ gives -0.00137 with $[-0.00180, -0.00110]$. Lower patience $\beta = 0.94$ gives 0.13629 with $[0.11113, 0.14976]$ and lower $r = 0.02$ gives 0.07253 with $[0.05591, 0.08221]$. Holding the calibration fixed and shifting target windows gives $[0.00090, 0.01444]$ for ages 20 to 29 versus 40 to 49, the focal $[-0.00819, -0.00298]$, and $[-0.00929, -0.00516]$ for ages

30 to 39 versus 50 to 59.

Table 7: Grid refinement and tolerance-first matching diagnostics

Panel A. Asset-grid refinement

Asset points	Mean $\lvert\Delta \log v\rvert$	95th percentile $\lvert\Delta \log v\rvert$	Mean wedge	95th percentile wedge	$\widehat{\mathfrak{G}}$	$\widehat{\mathfrak{D}}$
250	0.0006	0.0033	1.0120	1.0842	3.036	5.500
800	0.0004	0.0017	1.0119	1.0839	3.027	5.231
1200	0.0003	0.0013	1.0118	1.0834	3.023	5.195

Panel B. Tolerance-first current-cell graph

Tolerance ε	Exhaustive cap K	Exhaustive?	Mean mismatch	95th percentile mismatch	Candidate support share	Interval
0.001	24	yes	0.00042	0.00094	0.5686	$[-0.00374,\ -0.00350]$
0.002	34	yes	0.00088	0.00188	0.7438	$[-0.00664,\ -0.00506]$
0.005	58	yes	0.00231	0.00471	0.8993	$[-0.00819,\ -0.00298]$
0.010	82	yes	0.00475	0.00942	0.9268	$[-0.01055,\ -0.00219]$

Notes. Panel B fixes the tolerance band. The candidate support share is computed on the graph admitted by that band, not on the target domain alone. $\widehat{\mathfrak{G}}$ is the finite log spread of the recovered multipliers within a fiber; $\widehat{\mathfrak{D}}$ is the corresponding transport distance across ages. The cap K is the first value at which the search has reached all retained pairs. The maintained row sets $\varepsilon = 0.005$.

For the maintained row, the result is not a near miss. At $\varepsilon = 0.005$, the anchored finite program is feasible, and the parallel, cycle, band, and relaxation diagnostics are all zero at the reported precision. The borrowing kink audit then removes target cells whose common support depends on the lower bound. Retained focal support falls from 0.7472 to 0.7177, and the certified interval becomes $[-0.00159, 0.00090]$. The estimand supported by the sample has changed; the finite grid has not failed. The exercise isolates dependence on support at the boundary from numerical infeasibility or noise in the raw Euler equations.

The exercise with liquid and illiquid assets yields overlap 0.8151 on the fine $k \times \varepsilon$ grid and 0.8946 when assets are grouped into terciles and earnings are matched. The corresponding mean and worst contamination are 6.71 and 28.47 percent log points. The point summaries are $\Delta_{AB} = -0.2706$ with asset terciles and earnings, 1.7445 with earnings alone, and 0.9560 with age alone. The corresponding graph intervals are $[-3.2369, 6.7702]$, $[-4.1160, 7.9730]$, and $[-1.5240, 6.9176]$ percent log points. Since all three intervals contain 0, the richer state space does not certify a stronger sign. The fallback is the rule described above: a match at distance δ is allowed only after the bounds are widened by the declared interpolation allowance $L\delta$.

9 Conclusion

Local social discounting with rich heterogeneity begins by specifying who is being compared. The current matching rule fixes the represented self-transfer margin, the information that prices that margin apart from age, and the private marginal value used as the common unit. On supported exact matches, a comparison in physical resources isolates residual social priority. The graph theorem then gives the discipline: imposed local discount labels can be represented by positive residual multipliers only when parallel witnesses agree and cycle sums vanish, with levels identified separately in each connected component.

The method is diagnostic and conditional. A full policy ranking requires assumptions about missing cells, support, units, bridges, and anchors across components. In heterogeneous life-cycle economies, comparisons by age alone can mix private marginal values, rely on unsupported matches, and conceal failures of the graph restrictions. The applied recipe is therefore to derive the current map from the represented margin, state the private unit, build the supported graph, report mismatch and component diagnostics, compute intervals before point summaries, and rebuild the graph whenever the unit or the represented margin changes.

The quantitative exercise shows that these requirements matter. The verified graph can change support and rematching enough to alter selected signs, while alternative units, raw Euler propagation, and richer state spaces can remove sign certification altogether. Such non-certification is not a failure of the method. It is the message of the audit: the maintained data, margin, unit, bridge, and support certify only the local social-discounting claims that the graph can sustain.

A Aggregating the Pairwise Restriction

This appendix section converts the pairwise restriction into exact-fiber spread, mismatch-adjusted bounds, and contamination from coarsening. Regular conditional laws exist because $\mathcal{X} = \mathcal{A} \times \mathcal{Z}$ and the comparison-map codomain are maintained standard Borel.

A.1 Spread as an aggregation of pairwise gaps

Let

$$\Psi_t(x) := (\chi_t(x), \upsilon_t(x)), \qquad \nu_t := \Psi_{t\#}\mu_t,$$

and fix a regular conditional law $\{\mu_{t,g}\}_g$ for $X_t \sim \mu_t$ given $\Psi_t(X_t) = g$.

Definition A.1 (Fiberwise and global demographic spread)**.** For date t and fiber value g, define

$$\mathfrak{G}_t(\eta \mid g) := \operatorname*{ess\,sup}_{\mu_{t,g}} \log \eta_t - \operatorname*{ess\,inf}_{\mu_{t,g}} \log \eta_t. \tag{55}$$

The global spread is

$$\mathfrak{G}_t(\eta) := \operatorname*{ess\,sup}_{g \sim \nu_t} \mathfrak{G}_t(\eta \mid g). \tag{56}$$

On finite-grids, these are ordinary within fiber ranges and their maximum. Thus $\mathfrak{G}_t(\eta) = 0$ iff full-fiber conditional residual age neutrality holds at date t; tuple-relative neutrality gives the lower-bound statements below without requiering unused cells in the fiber to be neutral.

Definition A.2 (Exact fiber admissible comparison system)**.** An *exact fiber admissible comparison system* anchored at t is a measurable subprobability kernel $K_t(g, \mathrm{d}\pi)$ from fiber values into bridge-verified comparison tuples such that, for ν_t almost everywhere g, either $K_t(g, \Pi) = 0$ or the normalized kernel is supported on tuples whose two current cells lie in fiber g and whose induced current old and current young marginals are absolutely continuous with respect to $\mu_{t,g}$. Unsupported fibers are assigned the zero kernel.

For such a system, set $\underline{g}_t(g; K_t) = 0$ when $K_t(g, \Pi) = 0$; otherwise define

$$\underline{g}_t(g; K_t) := \operatorname*{ess\,sup}_{\pi \sim K_t(g,\cdot)/K_t(g,\Pi)} [\log \mathcal{Q}(\pi) - \log \mathcal{D}^S(\pi)]_+ \tag{57}$$

This wedge-free profile is conservative. With a verified KKT wedge and bridge correction, replace the bracket by $[\log \mathcal{Q} - \log \mathcal{D}^S + \log \widetilde{\Lambda}]_+$. The numerics use the conservative object unless a wedge implementation is named. Define

$$\underline{g}_t(K_t) := \operatorname*{ess\,sup}_{g \sim \nu_t} \underline{g}_t(g; K_t). \tag{58}$$

Proposition A.3 (Fiberwise lower bound profile)**.** *Fix t and an exact fiber admissible comparison system K_t. Under Assumptions 3.1, 3.3, 4.1, 6.1, 6.12 and 6.17 and nonpaternalism on M,*

$$\mathfrak{G}_t(\eta \mid g) \geq \underline{g}_t(g; K_t) \qquad \textit{for } \nu_t \textit{ almost everywhere } g. \tag{59}$$

Corollary A.4 (Aggregated spread bound)**.** *Under the same assumptions,*

$$\mathfrak{G}_t(\eta) \geq \underline{g}_t(K_t). \tag{60}$$

Finite grids add approximation because exact equality of υ_t is typically unavailable. Proposition 7.12 gives the corresponding grid-refinement discipline when support and component structure are stable.

A.2 Approximate matching and contamination under coarsened maps

Let χ_t^* be the verified current-cell map and $\bar{\chi}_t = \phi_t \circ \chi_t^*$ a coarsening. And let $B_t : \mathbb{R}_+ \to \mathcal{B}_t$ bin the private envelope scale (the identity in exact applications, weighted $\log \upsilon$ bins in the numerics). Define

$$\bar{\Psi}_t(x) := (\bar{\chi}_t(x), B_t(\upsilon_t(x))), \qquad \bar{\nu}_t := \bar{\Psi}_{t\#}\mu_t,$$

and fix conditional laws $\bar{\mu}_{t,\bar{g}}$. The coarse fiber spread is

$$\mathfrak{G}_t^{\bar{\chi}}(\eta \mid \bar{g}) := \operatorname*{ess\,sup}_{\bar{\mu}_{t,\bar{g}}} \log \eta_t - \operatorname*{ess\,inf}_{\bar{\mu}_{t,\bar{g}}} \log \eta_t.$$

Definition A.5 (Operative coarse comparison system)**.** An *operative coarse comparison system* anchored at t and $\bar{\Psi}_t$ is a measurable subprobability kernel $\bar{K}_t(\bar{g}, \mathrm{d}\pi)$ into bridge-verified ordered tuples retaining the age ordering and future-leg condition of Definition 5.1, with both current cells in coarse fiber $\bar{g}$ and normalized current marginals absolutely continuous with respect to $\bar{\mu}_{t,\bar{g}}$ when $\bar{K}_t(\bar{g}, \Pi) > 0$. Unsupported coarse fibers receive zero mass. The term *comparison tuple* remains reserved for exact fiber objects.

All $\bar{K}_t$-essential suprema below normalize the relevant positive-mass section and equal 0 when it has zero mass.

For tuples in $\bar{K}_t$, define

$$\mathcal{H}(\pi) := \log \mathcal{Q}(\pi) - \log \mathcal{D}^S(\pi) + \log \widetilde{\Lambda}(\pi), \tag{61}$$

ages $a^{\mathrm{y}}(\pi), a^{\mathrm{o}}(\pi)$, and mismatch

$$\varepsilon(\pi) := |\log \upsilon_t(x_t^{\mathrm{o}}) - \log \upsilon_t(x_t^{\mathrm{y}})|. \tag{62}$$

For every such tuple the coarse-domain pairwise algebra gives

$$\log \frac{\eta_t(x_t^{\mathrm{y}})}{\eta_t(x_t^{\mathrm{o}})} \geq \mathcal{H}(\pi) - \varepsilon(\pi), \tag{63}$$

by the raw identity in Proposition 5.6 and the represented bridge $\mathcal{R}^S = \mathcal{Q}\widetilde{\Lambda}$. The age-pair-conditioned mismatch-adjusted profile is

$$\underline{g}_t^{\varepsilon}(a^{\mathrm{y}}, a^{\mathrm{o}}, \bar{g}; \bar{K}_t) := \operatorname*{ess\,sup}_{\pi \sim \bar{K}_t(\bar{g},\cdot):\, a^{\mathrm{y}}(\pi)=a^{\mathrm{y}},\, a^{\mathrm{o}}(\pi)=a^{\mathrm{o}}} [\mathcal{H}(\pi) - \varepsilon(\pi)]_+, \tag{64}$$

with value 0 when the age pair is absent.

Definition A.6 (Approximate sufficiency of a coarsened comparison map)**.** A coarsening $\bar{\chi}_t$ is *κ-approximately sufficient* relative to $\bar{K}_t$ if there is a measurable age-pair-conditioned benchmark $\bar{h}_t$ and $\kappa \geq 0$ such that

$$|\mathcal{H}(\pi) - \bar{h}_t(a^{\mathrm{y}}(\pi), a^{\mathrm{o}}(\pi), \bar{g})| \leq \kappa \tag{65}$$

for $\bar{\nu}_t$ almost everywhere $\bar{g}$ and $\bar{K}_t(\bar{g}, \cdot)$ almost everywhere π.

Define

$$\bar{\varepsilon}_t(a^{\mathrm{y}}, a^{\mathrm{o}}, \bar{g}) := \operatorname*{ess\,sup}_{\pi \sim \bar{K}_t(\bar{g},\cdot):\, a^{\mathrm{y}}(\pi)=a^{\mathrm{y}},\, a^{\mathrm{o}}(\pi)=a^{\mathrm{o}}} \varepsilon(\pi), \tag{66}$$

again 0 if the age pair is absent. Let $\widetilde{\Psi}_t(\pi) := (a^{\mathrm{y}}(\pi), a^{\mathrm{o}}(\pi), \bar{\Psi}_t(x_t^{\mathrm{y}}))$ and let $\widetilde{\nu}_t^{\bar{K}}$ be the finite pushforward measure induced by $\bar{\nu}_t(\mathrm{d}\bar{g})\bar{K}_t(\bar{g}, \mathrm{d}\pi)$; if its total mass is 0, the following statements are vacuous.

Proposition A.7 (Coarsening contamination bound)**.** *If $\bar{\chi}_t$ is κ-approximately sufficient relative to $\bar{K}_t$, then under the maintained global assumptions and nonpaternalism on M,*

$$\mathfrak{G}_t^{\bar{\chi}}(\eta \mid \bar{g}) \geq [\bar{h}_t(a^{\mathrm{y}}, a^{\mathrm{o}}, \bar{g}) - \bar{\varepsilon}_t(a^{\mathrm{y}}, a^{\mathrm{o}}, \bar{g}) - \kappa]_+ \tag{67}$$

for $\widetilde{\nu}_t^{\bar{K}}$ *almost everywhere* $(a^{\mathrm{y}}, a^{\mathrm{o}}, \bar{g})$*. Consequently,*

$$\operatorname*{ess\,sup}_{(a^{\mathrm{y}},a^{\mathrm{o}},\bar{g})\sim\widetilde{\nu}_t^{\bar{K}}} \mathfrak{G}_t^{\bar{\chi}}(\eta \mid \bar{g}) \geq \operatorname*{ess\,sup}_{(a^{\mathrm{y}},a^{\mathrm{o}},\bar{g})\sim\widetilde{\nu}_t^{\bar{K}}} [\bar{h}_t(a^{\mathrm{y}}, a^{\mathrm{o}}, \bar{g}) - \bar{\varepsilon}_t(a^{\mathrm{y}}, a^{\mathrm{o}}, \bar{g}) - \kappa]_+. \tag{68}$$

Relative to Corollary 7.10, κ *is the extra loss from coarsening the current map.*

Remark A.8 (Operational sign certification). A comparison system is sign-informative only when Equation (67) is strictly positive on operative fibers and the finite graph has a nonempty feasible potential set. Report overlap, mismatch, contamination, edge/component counts, feasibility or cycle/parallel-label residuals, and interval width; if the interval contains 0, refine the grid or partition, or declare non-certification.

Corollary A.9 (Primitive Lipschitz control of contamination)**.** *Suppose there is a metric* d_t *on omitted current state objects and* $L_t < \infty$ *such that tuples* π, π' *in the same coarse fiber and age pair satisfy*

$$|\mathcal{H}(\pi) - \mathcal{H}(\pi')| \leq L_t d_t(\pi, \pi').$$

This is primitive in omitted current-state traits only when the candidate social discount schedule and KKT wedge have separate Lipschitz control; otherwise it is a regularity assumption on composite $\mathcal{H}$*.*

Let

$$\Delta_t(a^{\mathrm{y}}, a^{\mathrm{o}}, \bar{g}) := \sup\{d_t(\pi, \pi') : \pi, \pi' \text{ lie in the support of } \bar{K}_t(\bar{g}, \cdot),$$
$$a^{\mathrm{y}}(\pi) = a^{\mathrm{y}}(\pi') = a^{\mathrm{y}}, \quad a^{\mathrm{o}}(\pi) = a^{\mathrm{o}}(\pi') = a^{\mathrm{o}}\},$$

with value 0 *when empty. Then* $\bar{\chi}_t$ *is* κ*-approximately sufficient for any*

$$\kappa \geq \operatorname*{ess\,sup}_{(a^{\mathrm{y}},a^{\mathrm{o}},\bar{g})\sim\widetilde{\nu}_t^{\bar{K}}} \frac{1}{2} L_t \Delta_t(a^{\mathrm{y}}, a^{\mathrm{o}}, \bar{g}).$$

Section 8 reports support, mismatch, contamination, diagnostic envelopes, and maintained point-summary diagnostics in that order; the replication outputs retain the fuller partition diagnostic.

B Proofs and Technical Lemmas

This appendix collects algebra used outside the main text. Maintained primitives are Assumptions 3.1, 3.3, 4.1, 6.1, 6.12 and 6.17; result-specific hypotheses are added when invoked. Conditional objects

are on positive support.

B.1 Numerical accuracy and replication diagnostics

The replication archive records the environment, run records, and generated table sources. The manuscript reports the diagnostics needed for the local audit: grid refinement, private-unit mismatch, current-map dispersion, boundary classification, KKT wedge moments, bridge thresholds, raw-Euler stress rows, graph feasibility, bands, cycles, components, and minimal relaxation. The raw-Euler row in Table 6 is a stress test; the maintained wedge is the KKT-consistent projection.

B.2 Regularity

The proofs use measurability of comparison maps, continuation correspondences, and state-price kernels; existence of the stated derivatives; and regular conditional probabilities for Section A. Standard Borel structure supplies the last step.

Lemma B.1 (Standard Borel disintegration)**.** *Let $\Psi_t(x) = (\chi_t(x), \upsilon_t(x))$ be measurable from a standard Borel space $\mathcal{X}$ to a standard Borel codomain $\mathcal{U} \times \mathbb{R}_+$. Then there is a regular conditional law $\{\mu_{t,g}\}_g$ for $X_t \sim \mu_t$ given $\Psi_t(X_t) = g$, unique for $\nu_t := \Psi_{t\#}\mu_t$ almost every g, and*

$$\int f(x)\mu_t(\mathrm{d}x) = \int \left[\int f(x)\mu_{t,g}(\mathrm{d}x)\right] \nu_t(\mathrm{d}g)$$

for every integrable measurable f.

Proof. This is the standard regular conditional probability theorem for standard Borel spaces, followed by the law of iterated expectations. □

B.3 Verification of current maps and bridges

Proof of Proposition 4.9. Part (i) is margin sufficiency. For (ii), merging distinct verified codes destroys inherited sufficiency; the coarsening either fails on merged support points or requires a new check. Part (iii) follows because equality of (χ_t^M, W_t) implies equality of χ_t^M, and adding W_t only removes matches. □

Proof of Proposition 6.6. Fix an age and transition-row class, and let $w_a(b, \varepsilon_k) = y_a(\varepsilon_k) + (1 + r)b$. The continuation problem and one-step risk-free leg are the same scalar problem in w_a. Strict monotonicity of υ_a in w_a makes equal υ_a recover equal w_a, hence the same next asset and loading. Different transition rows use different Euler weights, so coarsening across rows requires a separate check; distinct rows give the earnings state. □

Proof of Corollary 6.14. Apply Proposition 6.13 to the convex two-asset problem. The tuple augments liquid state with illiquid holdings and adjustment-cost derivatives; liquid and illiquid KKT multipliers enter through loadings. Convexity gives the supporting-price inequality, slackness gives the wedge-free private case, and Assumptions 6.1 and 6.12 plus nonpaternalism give the social equality as in Proposition 6.18. □

Proof of Lemma 4.14. Continuity and strict monotonicity make each $b \mapsto \upsilon_t(a, b, u)$ one-to-one onto an interval. Any value in the overlap has one preimage at each age, producing a shared current fiber (u, v). Admissibility of a comparison tuple is the additional continuation-support condition imposed later in Definition 5.1. □

Proof of Proposition 6.13. For a gross future leg R, the private derivative is

$$-\upsilon_t(x_t^{\mathrm{y}}) + \frac{R}{\mathcal{Q}(\pi)} \left(\upsilon_t(x_t^{\mathrm{y}}) - \sum_j \lambda_j(\pi)\alpha_j(\pi) \right).$$

Setting it to 0 gives Equation (26). Positivity of the bracket is the admissibility condition $\sum_j \lambda_j(\pi)\alpha_j(\pi) < \upsilon_t(x_t^{\mathrm{y}})$; $\Xi(\pi) := \sum_j \lambda_j(\pi)\alpha_j(\pi)$ is the reduced-form KKT loading. □

Lemma B.2 (Private compensation representation)**.** *For a represented family that removes one current unit and adds a priced future leg, the private indifference factor is $\widehat{R}^P(\pi) = \mathcal{Q}(\pi)\Lambda(\pi)$ with $\Lambda(\pi) \geq 1$. Equality holds exactly when $\Xi(\pi) = 0$; locally spanned slack perturbations have this property, and strict loading/complementarity within that class gives the converse.*

Proof. This is Proposition 6.13 with $\Lambda(\pi) = [1 - \Xi(\pi)/\upsilon_t(x_t^{\mathrm{y}})]^{-1}$. □

Proof of Proposition 6.18. Lemma B.2 gives $\widehat{R}^P = \mathcal{Q}\Lambda$. Nonpaternalism and Assumption 6.12 identify this factor with $\mathcal{R}^S$, so $\mathcal{R}^S = \mathcal{Q}\Lambda \geq \mathcal{Q}$. Equality requires $\Xi = 0$; locally spanned slack perturbations are the primitive wedge-free case, with strict complementarity giving the converse. □

Proof of Corollary 6.22. If the leg is locally purchasable at state-price $q_{t,s}$, then $\mathcal{Q}(\pi) = q_{t,s}(x_s^{\mathrm{o}} \mid x_t^{\mathrm{y}})^{-1}$. Substitute this into Equation (28). The equality statement is the equality statement in Proposition 6.18. □

Proof of Proposition 6.20. By Proposition 4.7, each derivative equals its PVEU target integral minus the common financing integral. Subtracting cancels financing and gives Equation (29). Equal target mass makes the sign the sign of target-average differences. □

Proof of Proposition 8.2. Decompose the signed target measure over S and S^c. The S term is identified; omitted mass can overturn signs. Bounds $\eta_t \in [\underline{\eta}, \overline{\eta}]$ give the displayed sharp outer interval by assigning endpoints to omitted A and B mass. □

B.4 Pairwise algebra and graph restrictions

Proof of Proposition 5.6. Start from $\mathcal{D}^S = (\omega_t(x_t^{\mathrm{o}})/\omega_t(x_t^{\mathrm{y}}))\mathcal{R}^S$ and substitute $\omega_t = \eta_t \upsilon_t$ without canceling υ_t. Taking logs gives Equation (13). □

Proof of Corollary 5.7. The mismatch assumption bounds the last term in Equation (13) between $-\varepsilon$ and ε. □

Proof of Proposition 5.8. Normalize $\omega_s(x_s^{\mathrm{o}}) = \omega_t(x_t^{\mathrm{o}}) = \upsilon_t(x_t^{\mathrm{y}}) = 1$, set $\omega_t(x_t^{\mathrm{y}}) = e^{\gamma}$ and $\upsilon_t(x_t^{\mathrm{o}}) = e^{-\delta}$, and take $\delta > \gamma > 0$. Then Equation (13) gives residual log ratio $\gamma - \delta < 0$, while an exact fiber has private-scale ratio one and residual log ratio $\gamma > 0$. □

Proof of Corollary 5.9. Apply Proposition 5.5 block by block and multiply. Singleton future legs linked to the next older current cell cancel intermediate welfare weights and give the endpoint ratio; portfolio legs need not. Product bounds and log-error addition follow. □

Proof of Proposition 7.1. Proposition 5.5 gives $\eta_t(x_t^{\mathrm{y}})/\eta_t(x_t^{\mathrm{o}}) = \mathcal{R}^S(\pi)/\mathcal{D}^S(\pi)$. Proposition 6.18 sets $\mathcal{R}^S = \mathcal{Q}\Lambda$ in the baseline, yielding the displayed log equality; with bridge correction replace Λ by $\widetilde{\Lambda}$. Since $\Lambda \geq 1$, $\mathcal{D}^S < \mathcal{Q}$ implies positive residual tilt, contradicting neutrality on that fiber. □

Proof of Proposition 7.4. This is the displayed equality in the proof of Proposition 7.1, written as a directed edge weight. With $\mathfrak{B} \neq 1$, the same equality uses the corrected bridge relation $\mathcal{R}^S = \mathcal{Q}\Lambda\mathfrak{B}$. The weak lower bound that drops $\log \Lambda \geq 0$ is a baseline $\mathfrak{B} \equiv 1$ statement only. □

Proof of Theorem 7.5. Necessity is telescoping on closed walks. Same-edge witness labels must agree because each equals $\log \widetilde{\eta}(x^{\mathrm{y}}) - \log \widetilde{\eta}(x^{\mathrm{o}})$. Conversely, impose parallel-label consistency, anchor each component, and define $\log \widetilde{\eta}(x)$ as minus the signed $\bar{g}$ path sum from the anchor to x. Cycle consistency gives path independence; exponentiation yields positive multipliers, unique up to component constants. Countable/measurable graphs use the same construction under integrable path sums. □

Proof of Proposition 7.6. Proposition 7.4 writes each edge as the tail-head difference in $\log \eta$. Path sums telescope; cycles sum to 0; paths with common endpoints agree. A spanning-tree recursion with one anchor recovers the component potential, and changing the anchor rescales all levels by one constant. □

Proof of Corollary 7.7. Choose an anchor level in each component and assign every other level by summing exact edge weights along any path from the anchor. Proposition 7.6 makes the assignment path independent. A different anchor multiplies all component levels by the same constant, leaving ratios unchanged. □

Proof of Corollary 7.10. Combine Corollary 5.7 with $\mathcal{R}^S = \mathcal{Q}\widetilde{\Lambda}$ to get $\log(\eta_t(x_t^{\mathrm{y}})/\eta_t(x_t^{\mathrm{o}})) \geq \log \mathcal{Q} - \log \mathcal{D}^S + \log \widetilde{\Lambda} - \varepsilon$. The stated sufficient condition makes the right side positive; in the baseline, dropping $\log \Lambda \geq 0$ gives the simpler sufficient condition. □

Proof of Proposition 7.11. For each approximate edge, Assumption 6.12 and proposition 6.18 give $\widetilde{g}_t^{\ell} = \log \omega_t(x^{\ell-1}) - \log \omega_t(x^{\ell})$. Sums telescope, so endpoint-equivalent chains agree. Since $\omega_t = \eta_t \upsilon_t$, the residual-multiplier error is the endpoint private-scale difference, bounded by the edge mismatches sum. □

Proof of Corollary 7.15. If nonpaternalism holds and $\mathcal{D}^S < \mathcal{Q}$ on positive measure, Proposition 7.1 forces positive residual age tilt, contradicting neutrality. Conversely, nonpaternalism plus neutrality sets the leftside of Equation (30) to 0, so $\mathcal{D}^S = \mathcal{Q}\Lambda \geq \mathcal{Q}$ almost everywhere □

B.5 Aggregation, contamination, and computation

Proof of Proposition A.3. For every tuple in fiber g, Proposition 7.1 gives Equation (30). Absolute continuity of the current marginals with respect to $\mu_{t,g}$ bounds the right side by the within-fiber

essential range of $\log \eta_t$; taking the tuple essential supremum gives the result. □

Proof of Corollary A.4. Take the essential supremum of Equation (59) over $g \sim \nu_t$. □

Proof of Proposition A.7. Apply Equation (63). Approximate sufficiency loses at most κ and mismatch at most $\bar{\varepsilon}_t$; the two current cells lie in one coarse fiber, whose spread bounds the left side. Positive parts and essential suprema give the displays. □

Proof of Corollary A.9. Within a fixed coarse fiber and age pair, $\mathcal{H}$ oscillates by at most $L_t\Delta_t$. Taking the midpoint as $\bar{h}_t$ puts every value within half that oscillation, yielding the displayed admissible κ. □

Proof of Proposition 8.1. Let S be the continuation marginal-utility sum. The Euler equation $u'(c_a) = \beta p_a(1+r)S + \lambda_a(i,k)$ and the derivative $-u'(c_a) + \beta p_a RS$ give $\widehat{R}_a^P = (1+r)\Lambda_a^{(i,k)}$, with $\Lambda_a^{(i,k)} = [1 - \lambda_a(i,k)/u'(c_a)]^{-1} \geq 1$ and $\mathcal{Q}_a^{(i,k)} = 1+r$. Propositions 5.6 and 6.18 imply the claim. □

Proof of Proposition 7.12. After component anchoring, the finite program is a closed system of edge-band inequalities. Assumptions (i) to (iv) give outer convergence of constraints, labels, and target weights, exclude persistent spurious constraints, and keep feasible sets compact. Assumption (v) gives nonemptiness and inner convergence, ruling out vanishing-cycle artifacts. Hence anchored feasible potential sets converge in Hausdorff distance. The target functional in Equation (51) is continuous on the common compact envelope, so the interval follows by the maximum and minimum theorem. □

Data and code availability. The replication files are available at https://github.com/sbuhai/current-cell-matching-project; no restricted data are used.

References

Afriat, S.N., "The Construction of Utility Functions from Expenditure Data," *International Economic Review* 8 (1967), 67-77.

Aiyagari, S.R., "Uninsured Idiosyncratic Risk and Aggregate Saving," *Quarterly Journal of Economics* 109 (1994), 659-684.

Arias, E., J. Xu and K.D. Kochanek, "United States Life Tables, 2021," *National Vital Statistics Reports* 72 (2023), no. 12.

Baqaee, D.R., A.T. Burstein and Y. Koike-Mori, "Measuring Welfare by Matching Households across Time," *Quarterly Journal of Economics* 139 (2024), 533-573.

Barcons, S., E. Dávila and A. Schaab, "Intergenerational Welfare Assessments," NBER Working Paper No. 34616, 2026.

Calvo, G.A. and M. Obstfeld, "Optimal Time-Consistent Fiscal Policy with Finite Lifetimes," *Econometrica* 56 (1988), 411-432.

Caplin, A. and J.V. Leahy, "The Social Discount Rate," *Journal of Political Economy* 112 (2004), 1257-1268.

Conesa, J.C. and D. Krueger, "Social Security Reform with Heterogeneous Agents," *Review of Economic Dynamics* 2 (1999), 757-795.

Dávila, E. and A. Schaab, "Welfare Assessments with Heterogeneous Individuals," *Journal of Political Economy* 133 (2025), 2918-2961.

Eden, M., "The Cross-Sectional Implications of the Social Discount Rate," *Econometrica* 91 (2023), 2065-2088.

Farhi, E. and I. Werning, "Inequality and Social Discounting," *Journal of Political Economy* 115 (2007), 365-402.

Feng, T. and S. Ke, "Social Discounting and Intergenerational Pareto," *Econometrica* 86 (2018), 1537-1567.

Gourinchas, P.-O. and J.A. Parker, "Consumption over the Life Cycle," *Econometrica* 70 (2002), 47-89.

Harsanyi, J.C., "Cardinal Welfare, Individualistic Ethics, and Interpersonal Comparisons of Utility," *Journal of Political Economy* 63 (1955), 309-321.

Heckman, J.J., H. Ichimura and P.E. Todd, "Matching as an Econometric Evaluation Estimator: Evidence from Evaluating a Job Training Programme," *Review of Economic Studies* 64 (1997), 605-654.

Hendren, N. and B. Sprung-Keyser, "A Unified Welfare Analysis of Government Policies," *Quarterly Journal of Economics* 135 (2020), 1209-1318.

Howarth, R.B. and R.B. Norgaard, "Intergenerational Transfers and the Social Discount Rate," *Environmental and Resource Economics* 3 (1993), 337-358.

Huggett, M., "The Risk-Free Rate in Heterogeneous-Agent Incomplete-Insurance Economies," *Journal of Economic Dynamics and Control* 17 (1993), 953-969.

Imbens, G.W. and J.M. Wooldridge, "Recent Developments in the Econometrics of Program

Evaluation," *Journal of Economic Literature* 47 (2009), 5-86.

Karp, L. and A. Rezai, "The Political Economy of Environmental Policy with Overlapping Generations," *International Economic Review* 55 (2014), 711-733.

Mertens, J.-F. and A. Rubinchik, "Intergenerational Equity and the Discount Rate for Policy Analysis," *Macroeconomic Dynamics* 16 (2012), 61-93.

Millner, A. and G. Heal, "Choosing the Future: Markets, Ethics, and Rapprochement in Social Discounting," *Journal of Economic Literature* 61 (2023), 1037-1087.

Rockafellar, R.T., *Convex Analysis*, Princeton: Princeton University Press, 1970.

Saez, E. and S. Stantcheva, "Generalized Social Marginal Welfare Weights for Optimal Tax Theory," *American Economic Review* 106 (2016), 24-45.

Schneider, M.T., C.P. Traeger and R. Winkler, "Trading off Generations: Equity, Discounting, and Climate Change," *European Economic Review* 56 (2012), 1621-1644.

Sher, I., "Generalized Social Marginal Welfare Weights Imply Inconsistent Comparisons of Tax Policies," *American Economic Review* 114 (2024), 3551-3577.

Varian, H.R., "The Nonparametric Approach to Demand Analysis," *Econometrica* 50 (1982), 945-973.